Manonmaniam Sundaranar University,
Directorate of Distance & Continuing
Education, Tirunelveli - 627 012
Tamilnadu, India

OPEN AND DISTANCE LEARNING (ODL) PROGRAMMES

(FOR THOSE WHO JOINED THE PROGRAMMES FROM THE ACADEMIC YEAR 2023–2024)

M.Sc. Physics

Course Material

ADVANCED OPTICS

SPHE21

Prepared

By

Dr. V. Sabarinathan

Department of Physics
Manonmaniam Sundaranar University
Tirunelveli - 12

ADVANCED OPTICS

UNITS	DETAILS
I	**POLARIZATION AND DOUBLE REFRACTION**: Classification of polarization – Transverse character of light waves – Polarizer and analyzer – Malu's law – Production of polarized light –Wire grid polarizer and the polaroid – Polarization by reflection – Polarization by double refraction – Polarization by scattering – The phenomenon of double refraction – Normal and oblique incidence – Interference of polarized light: Quarter and half wave plates – Analysis of Polarized light–Optical activity
II	**LASERS**: Basic principles – Spontaneous and stimulated emissions – Components of the laser – Resonator and lasing action – Types of lasers and its applications – Solid state lasers – Ruby laser – Nd: YAG laser – gas lasers –He-Ne laser–CO_2laser–Chemicallasers–HCl laser–Semiconductor laser.
III	**FIBEROPTICS**: Introduction – Total internal reflection – The optical fiber – Glass fibers – The coherent bundle – The numerical aperture – Attenuation in optical fibers – Single and multi-mode fibers – Pulse dispersion in multimode optical fibers –Ray dispersion in multimode step index fibers –Parabolic- index fibers – Fiber-optic sensors: precision n displacement sensor– Precision vibration sensor
IV	**NON-LINEAR OPTICS**: Basic principles – Harmonic generation – Second harmonic generation – Phase matching – Third harmonic generation – Optical mixing – Parametric generation of light – Self-focusing of light.
V	**MAGNETO- OPTICS AND ELECTRO-OPTICS:** Magneto - optical effects – Zeeman effect – Inverse Zeeman effect – Faraday effect – Voigt effect – Cotton-mouton effect – Kerr magneto- optic effect – Electro-optical effects – Stark effect – Inverse stark effect – Electric double refraction – Kerr electro – optic effect–Pockels electro-optic effect.
Recommended Text	
1	B. B. Laud, 2017, Lasers and Non – Linear Optics, 3rd Edition, New Age International (P) Ltd.
2	Ajoy Ghatak, 2017, Optics, 6th Edition, McGraw – Hill Education Pvt. Ltd.
3	WilliamT.Silfvast,1996, Laser Fundamentals Cambridge University Press, New York
4	J. Peatros, Physics of Light and Optics, a good (and free!) electronic book.
5	B. Saleh, and M. Teich, Fundamentals of Photonics, Wiley- Inter science,

UNIT – I
POLARIZATION AND DOUBLE REFRACTION

Classification of polarization

Light in the form of a plane wave in space is said to be linearly polarized. Light is a transverse electromagnetic wave, but natural light is generally unpolarized, all planes of propagation being equally probable. If light is composed of two plane waves of equal amplitude by differing in phase by 90°, then the light is said to be circularly polarized. If two plane waves of differing amplitude are related in phase by 90°, or if the relative phase is other than 90° then the light is said to be elliptically polarized.

The three major classification of polarization,

- Linear Polarization
- Circularly Polarization
- Elliptically Polarization

Linear Polarization

A plane electromagnetic wave is said to be linearly polarized. The transverse electric field wave is accompanied by a magnetic field wave as shown in Fig 1.1.

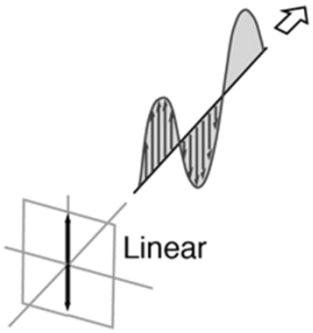

Fig 1.1 Linear polarization of light

Circularly Polarization

Circularly polarized light consists of two perpendicular electromagnetic plane waves of equal amplitude and 90° difference in phase. The light illustrated is right- circularly polarized.

If light is composed of two plane waves of equal amplitude but differing in phase by 90°, then the light is said to be circularly polarized. If you could see the tip of the electric field vector, it would appear to be moving in a circle as it approached you. If while looking at the source, the electric vector of the light coming toward you appears to be rotating counterclockwise, the light is said to be right-circularly polarized. If clockwise, then left-circularly polarized light. The electric field vector makes one complete revolution as the light advances one wavelength toward you. Another way of saying it is that if the thumb of your right hand were pointing in the direction of propagation of the light, the electric vector would be rotating in the direction of your fingers.

Circularly polarized light may be produced by passing linearly polarized light through a

quarter-wave plate at an angle of 45° to the optic axis of the plate.

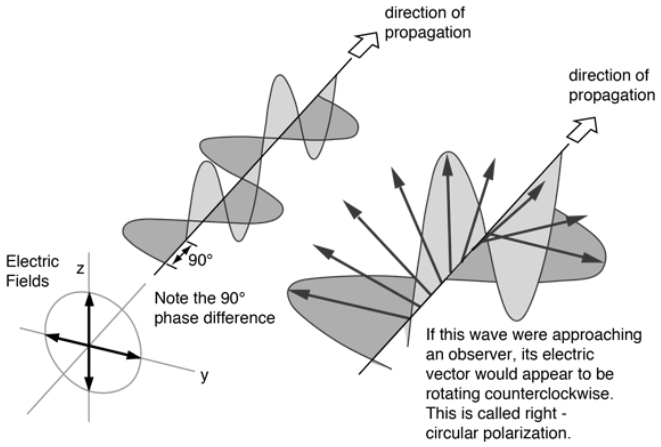

Fig 1.2 Circular polarization of light

Elliptically Polarization

Elliptically polarized light consists of two perpendicular waves of unequal amplitude which differ in phase by 90°. The Fig 1.3 shows right- elliptically polarized light.

If the thumb of your right hand were pointing in the direction of propagation of the light, the electric vector would be rotating in the direction of your fingers.

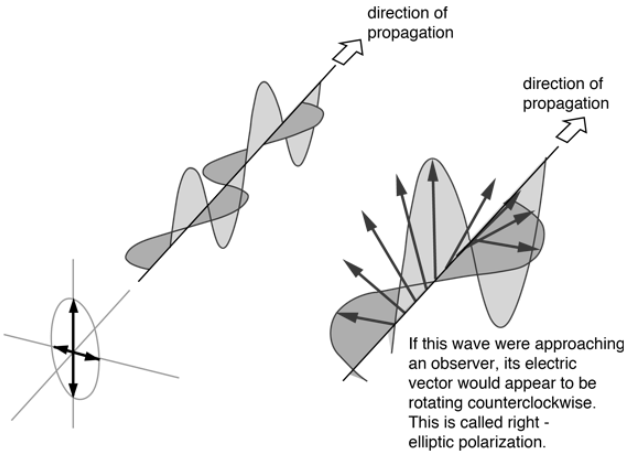

Fig 1.3 Elliptical polarization of light

Transverse character of light waves

A beam of unpolarized light is allowed to fall on the first tourmaline crystal. It is cut such that its optical axis Q_1A_1 is parallel to its surface. unpolarized light consists of vibrations in all directions. The light is transmitted by the plate T_1 is fully transmitted by the plate T_2, when their optical axes Q_1A_1 & Q_2A_2 are parallel to each other. When plate T_2 is gradually rotated with respective T_1, the Intensity of light transmitted by T_2 is decreased. And finally, the light transmitted by the crystal plate T_2 is completely cut off, when the optical axes Q_1A_1&

Q_2A_2 are perpendicular to each other. These vibrations are coming out perpendicular to the direction of propagation. This expt. proves the transverse nature of light, as shown in Fig 1.4.

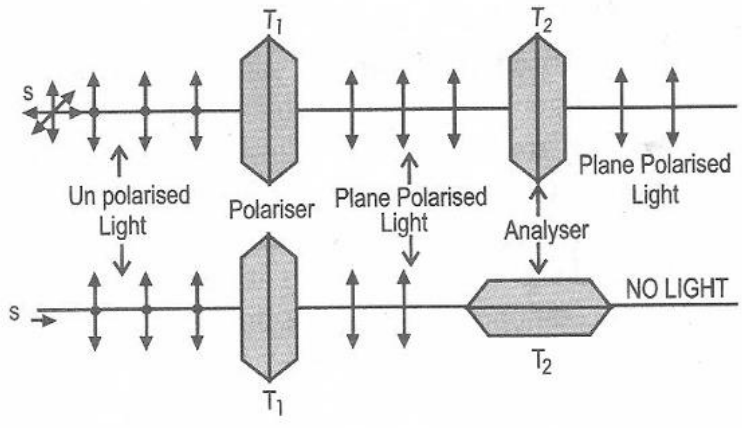

Fig 1.4 Polarization

Polarizer and analyzer

Polarizer: A polarizer is a material or device that selectively allows light waves oscillating in a particular plane to pass through while blocking or attenuating light waves oscillating in other planes. Essentially, it polarizes unpolarized light or aligns the polarization of polarized light.

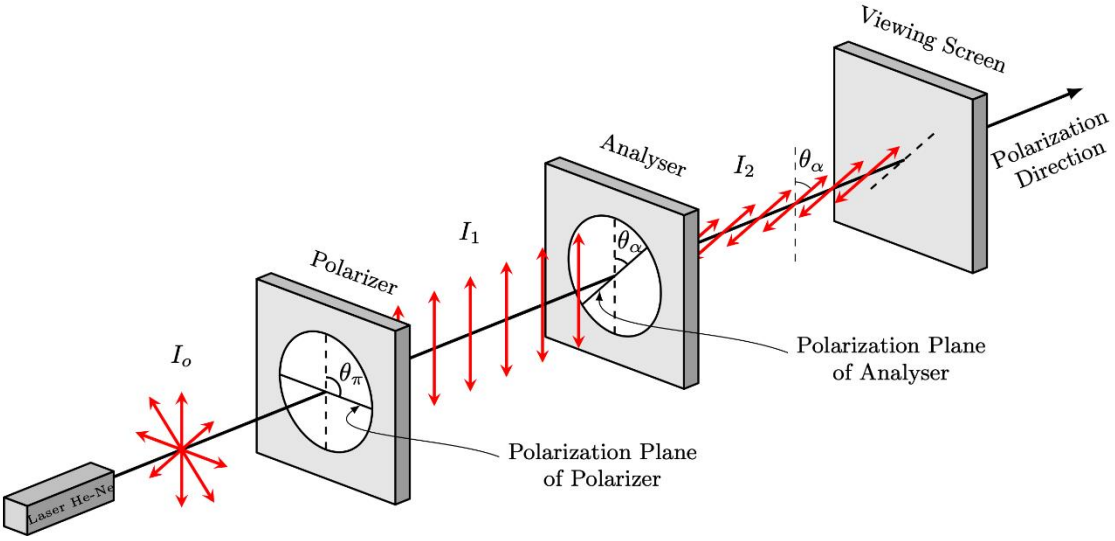

Fig 1.5 Polarizer and Analyzer

Analyzer: An analyzer is another polarizing material or device that is placed after the polarizer in an optical setup. It allows the detection or measurement of the polarization state of light that passes through it. By analyzing the light's polarization, it can provide information about the properties of the light source or the medium it has passed through.

Malu's law

The law describes how the intensity of light transmitted by the analyzer varies with the angle that its plane of transmission makes with that of the polarizer. The law can be stated in words as follows: The intensity of the transmitted light varies as the square of the cosine of the angle between the two planes of transmission.

If A_0 is the amplitude of the incident light and A_t is amplitude of the light transmitted through the analyzer, then

$$A_t=A_0\cos\theta$$

As we know the

$$\text{Intensity}\alpha\ (\text{amplitude})^2$$

Then,

$$I_t=A^2_t=A^2_0\cos^2\theta=I^2_0\cos^2\theta$$

Where;

I_t is the intensity of the light transmitted through the analyzer;

I^2_0 is the intensity of the incident plane polarized light.

Special cases

- If θ is zero, the second polarizer(analyzer)is aligned with the first polarizer, and the value of $\cos^2\theta$ is one. Thus, the intensity transmitted by these second filter is equal to the light intensity that passes through the first filter. This case will allow maximum intensity to pass through.
- If θ is 90˚, the second polarizer(analyzer) is oriented perpendicular to the plane of polarization of the first filter, and the $\cos^2(90^\circ)$ gives zero. Thus, no light is transmitted through the second filter. This case will allow minimum(zero)intensity to passthrough.

Production of polarized light

Polarized light can be produced by the following:

- Wire grid polarizer
- Polarization by reflection
- Polarization by double refraction
- Polarization by scattering

Wire grid polarizer and the polaroid

The physics behind the working of the wire grid polarizer is probably the easiest to understand. It essentially consists of a large number of thin copper wires placed parallel to each other as shown in Fig 1.6. When an unpolarized electromagnetic wave is incident on it then the component of the electric vector along the length of the wire is absorbed. This is due to the fact that the electric field does work on the electrons inside the thin wires and the energy associated with the electric field is lost in the Joule heating of the wires. On the other hand, (since the wires are assumed to be very thin) the component of the electric vector along the x-axis passes through without much attenuation. Thus, the emergent wave is linearly polarized with the electric vector along the x-axis. However, for the system to be effective (i.e., the E_y component almost completely attenuated) the spacing between the wires should be$\leq \lambda$, Clearly, the fabrication of such a polarizer for a 3 cm microwave is relatively easy. because the spacing has

to be < 3 cm.

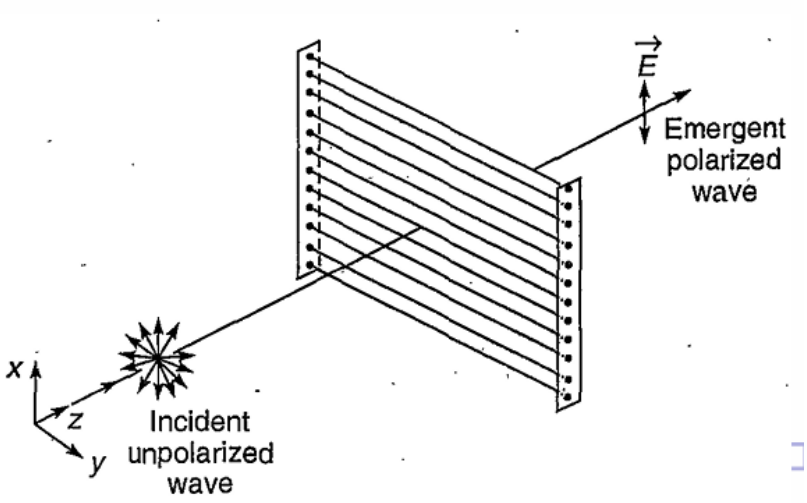

***Fig 1.6* Wire grid polarizer**

Polarization by reflection

When unpolarized natural light is incident on a reflecting surface between two transparent optical materials. For most angles of incidence, waves for which the electric-field vector is perpendicular to the plane of incidence (that is, parallel to the reflecting surface) are reflected more strongly than those for which lies in this plane. In this case the reflected light is partially polarized in the direction perpendicular to the plane of incidence. But at one particular angle of incidence, called the polarizing angle θ_p ($= \tan^{-1} n_2/n_1$) the light for which $\vec{E}$ lies in the plane of incidence is not reflected at all, but is completely refracted. At this same angle of incidence, the light for which is perpendicular to the plane of incidence is partially reflected and partially refracted. The reflected light is therefore completely polarized perpendicular to the plane of incidence, as shown in Fig. 1.7.a.

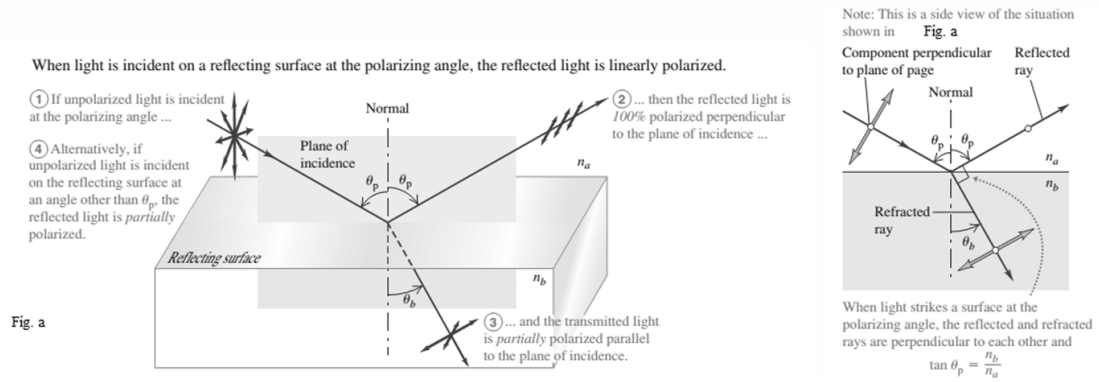

Fig 1.7 Polarization by reflection

Polarization by double refraction

When an unpolarized beam enters a dichroic crystal-like tourmaline, it splits up into two linearly polarized components. One of the components gets absorbed quickly and the other component passes through without much attenuation.

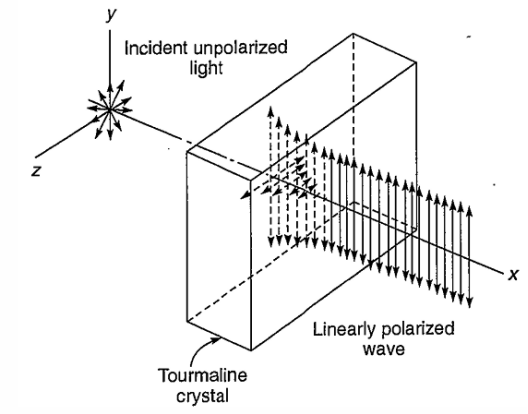

Fig 1.8 Polarization by double refraction

Polarization by scattering

The scattering of light off air molecules produces linearly polarized light in the plane perpendicular to the incident light. The scatterers can be visualized as tiny antennae which radiate perpendicular to their line of oscillation. If the charges in a molecule are oscillating along the y-axis, it will not radiate along the y-axis.

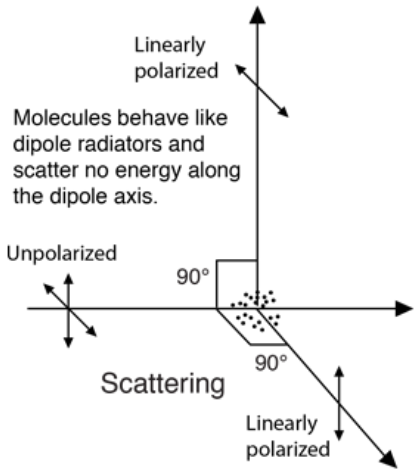

Fig 1.9 Polarization by scattering

Therefore, at 90° away from the beam direction, the scattered light is linearly polarized. This causes the light which undergoes Rayleigh scattering from the blue sky to be partially polarized.

The phenomenon of double refraction

The double refraction of light is the phenomenon of birefringence. It is an optical property in which a single ray of unpolarized light enters an anisotropic medium and splits into two rays, each travelling in a different direction. We can think of double refraction as the end which divides into two roads. Here, the end is the anisotropic medium, the person travelling is the unpolarized light, while the two roads are the two rays, each travelling their paths shown in Fig 1.10.

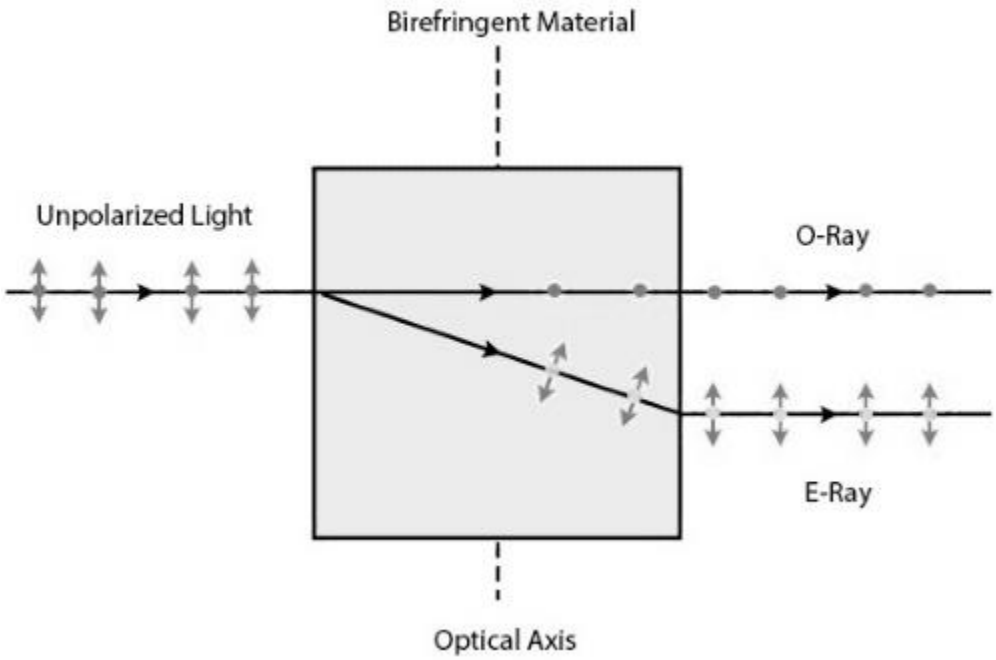

Fig 1.10 Double refraction of light

Birefringence is characterized by crystallographic materials with different recurrence indicators concerning different crystallographic directions. Birefringence occurs when light passes through transparent objects, ordered by molecules, indicating a differential difference in reception at refractive indices.

Normal and oblique incidence

Normal Incidence: This occurs when waves strike a surface perpendicularly, meaning the angle of incidence is 0 degrees. In this case, the incident wave is aligned directly with the normal vector to the surface. When waves encounter a surface at normal incidence, they typically undergo minimal reflection or refraction, depending on the properties of the surface.

Oblique Incidence: This occurs when waves strike a surface at an angle other than 0 degrees. The angle of incidence is measured between the incident wave and the normal vector to the surface. When waves encounter a surface at oblique incidence, they can reflect, refract, diffract, or absorb depending on the properties of the surface material and the angle of incidence.

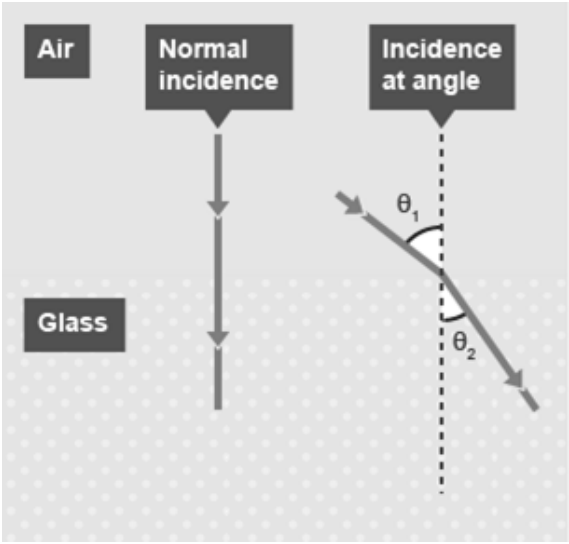

Fig 1.10.(b) Double refraction of light

Interference of polarized light:

Interference of polarized light refers to the phenomenon where two or more polarized light waves interact with each other, resulting in constructive or destructive interference patterns. Polarized light is light in which the electromagnetic waves oscillate predominantly in a specific direction. When polarized light waves overlap, their electric fields can either reinforce or cancel each other out, depending on their relative phase.

Constructive interference occurs when the peaks of one polarized light wave align with the peaks of another, resulting in an increase in the overall intensity of light at that point. Destructive interference occurs when the peaks of one wave align with the troughs of another, leading to a decrease in intensity or even cancellation of light at that point.

Quarter and half wave plates
Half wave plates:

A half wave plate tends to shift the polarization direction of linearly polarized light. When considering a linearly polarized light, a half wave plate refers to the effect of the half wave plate that rotates the polarization vector at an angle of 2θ. However, if we consider an elliptically polarized light, the half wave plate shows the effect of inverting the handedness of the light.

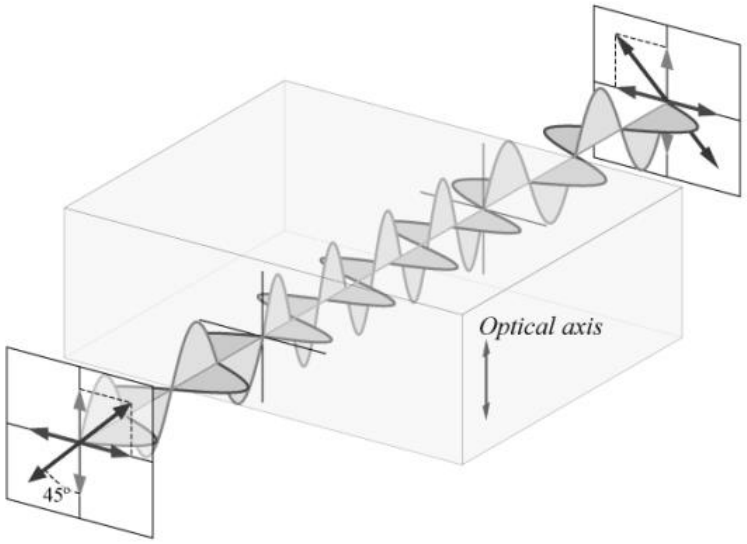

Fig 1.11(a) Half Wave Plate

For a half wave plate, we can use a relationship between L (thickness of the crystal), Δn (birefringence, the double refraction of light in a transparent, molecularly ordered material), and λ_0 (vacuum wavelength of the light). The relationship is as follows:

$$\Gamma = \frac{2\pi \Delta n L}{\lambda 0}$$

Γ is the amount of relative phase. For a half wave plate, the phase shift between polarization components can be given as $\Gamma = \pi$.

Quarter wave plates:

A quarter wave plate converts a linearly polarized light into circularly polarized light and vice versa. This type of wave plate is useful in producing an elliptical polarization as well.

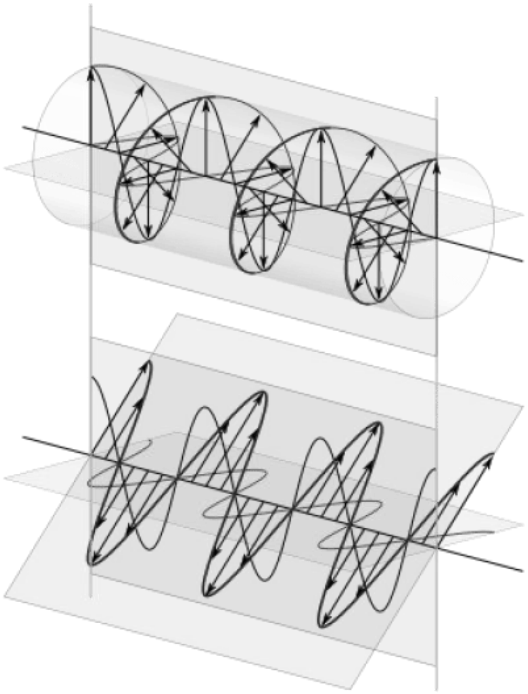

Fig 1.11(b) Quarter Wave Plate

In this type of wave plate, the polarization of the incoming photon is resolved into two polarizations at the x and y axis. Moreover, in this type of wave plate, the input polarization is parallel to the fast or slow axis. This results in no polarization of the other axis; thus, the output polarization is similar to the input. If the input polarization is about 45 degrees to the fast and slow axis, polarization tends to be equal at those axes.

Analysis of Polarized light

Analysis of polarized light Let a monochromatic light is incident on Nicole prism, after passing through it light is plane polarized and it is incident normally on double refracting crystal P (calcite or quartz). The plane polarized light entering into the crystal is split up into two components that is ordinary and extra ordinary. Both light components travel along the same direction but with different velocities. Let t be the thickness of this crystal which produces phase difference δ between ordinary and extra ordinary ray.

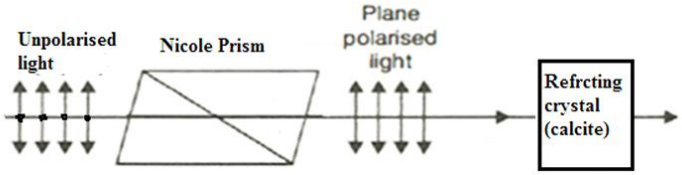

Fig 1.12 Polarized light analysis

Suppose the amplitude of the incident plane polarized light in a crystal is A and it makes an angle θ with the optic axis. Therefore, the amplitude of ordinary ray vibrating along PO is $Asin\theta$ and amplitude of extra ordinary ray vibrating along PE is $Acos\theta$. Since a phase difference δ is introduced between the two rays after passing through the thickness 't' of crystal, the rays coming out of the crystal can be represented in terms of two simple harmonic motions as

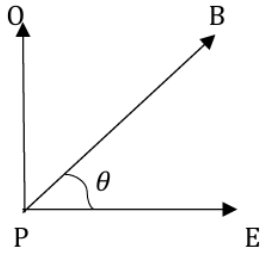

For extra ordinary ray, $x = Acos\theta \sin(\omega t + \delta)$

For ordinary ray, $y = Asin\theta \sin \omega t$

Let $Acos\theta = a \quad \& \quad Asin\theta = b$

$$x = a \sin(\omega t + \delta) \quad \ldots\ldots\ldots (1)$$

$$y = b \sin \omega t \quad \ldots\ldots\ldots (2)$$

From equation (2)

$$\frac{y}{b} = \sin \omega t \quad \ldots\ldots\ldots (3)$$

$$\cos \omega t = \sqrt{1 - \frac{y^2}{b^2}} \quad \ldots\ldots\ldots (4)$$

From equation (1)

$$\frac{x}{a} = \sin(\omega t + \delta)$$

$$\frac{x}{a} = \sin \omega t \cos \delta + \cos \omega t \sin \delta$$

From eqⁿ (3) & (4) above eqⁿ becomes

$$\frac{x}{a} = \frac{y}{b}\cos \delta + \sqrt{1 - \frac{y^2}{b^2}} \sin \delta$$

$$\frac{x}{a} - \frac{y}{b}\cos \delta = \sqrt{1 - \frac{y^2}{b^2}} \sin \delta$$

Squaring on both side, we get

$$\frac{x^2}{a^2} + \frac{y^2}{b^2}\cos^2 \delta - \frac{2xy}{ab}\cos \delta = \left(1 - \frac{y^2}{b^2}\right)\sin^2 \delta$$

$$\frac{x^2}{a^2}+\frac{y^2}{b^2}\cos^2\delta-\frac{2xy}{ab}\cos\delta=\sin^2\delta-\frac{y^2}{b^2}\sin^2\delta$$

$$\frac{x^2}{a^2}+\frac{y^2}{b^2}(\cos^2\delta+\sin^2\delta)-\frac{2xy}{ab}\cos\delta=\sin^2\delta \quad \ldots\ldots\ldots\ldots(5)$$

Special cases:

1) When $\delta = 0$

eqⁿ (5) becomes

$$\left(\frac{x}{a}-\frac{y}{b}\right)^2=0$$

$$\frac{y}{b}=\frac{x}{a}$$

$$y=\frac{b}{a}x$$

This gives the eqⁿ of straigh line . Therefore the emergent light is plane polarised.

2) When $\delta=\frac{\pi}{2}$ & $a\neq b$

eqⁿ (5) becomes

$$\frac{x^2}{a^2}+\frac{y^2}{b^2}=1$$

This represents the equation of a symmetrical ellipse. In this case the emergent light will be elliptically polarised provided $a \neq b$.

3) When $\delta=\frac{\pi}{2}$ & $a=b$

eqⁿ (5) becomes

$$x^2+y^2=a^2$$

This represents the equation of circle of radius a. In this case the emergent light will be circularly polarised.

Here in this case, the vibration of plane polarised light on the crystal makes an angle 45^0 with the direction of the optic axis.

Optical activity

The ability of substance (crystal or solution) to rotate plane of polarization about the direction of light is called as optical activity. The substance (crystal or solution) which can rotate plane polarized light is called as optical active substance.

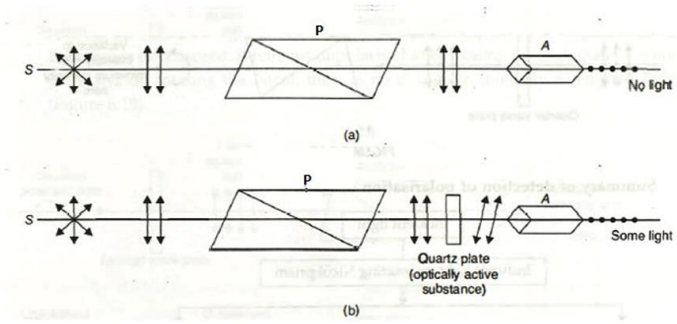

Fig 1.13 Optical activity

There are two types of optically active substance

1) **Dextro rotatory**
   The substance which rotates the plane of vibration in the clockwise with respect to the observer looking towards the source from the analyzer is called as Dextro rotatory (right-handed). Ex., Fruit Sugar, quartz crystal, etc.
2) **Laevo Rotatory**
   The substance which rotates the plane of vibration in the anticlockwise with respect to the observer looking towards the source from the analyzer is called as Laevo rotatory (lefthanded). Ex. Cane sugar solution

UNIT – II
LASERS

Basic principles

Population inversion

Atomic energy states are much more complex. There are many more energy levels, and each one has its own time constants for decay. The four-level energy diagram shown in Fig 2.1 is representative of some real lasers. The electron is pumped (excited) into an upper level E_4 by some mechanism (for example, a collision with another atom or absorption of high-energy radiation). It then decays to E_3, then to E_2, and finally to the ground state E_1. Let us assume that the time it takes to decay from E_2 to E_1 is much longer than the time it takes to decay from E_2 to E_1. In a large population of such atoms, at equilibrium and with a continuous pumping process, a population inversion will occur between the E_3 and E_2 energy states, and a photon entering the population will be amplified coherently.

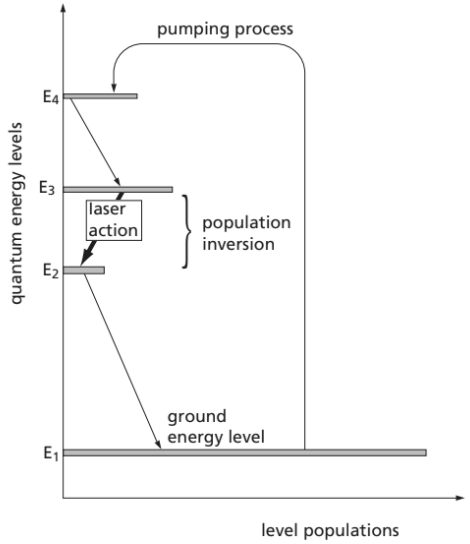

Fig 2.1 Four-level energy diagram

Spontaneous and stimulated emissions

In general, when an electron is in an excited energy state, it must eventually decay to a lower level, giving off a photon of radiation. This event is called "spontaneous emission," and the photon is emitted in a random direction and a random phase. The average time it takes for the electron to decay is called the time constant for spontaneous emission, and is represented by t. On the other hand, if an electron is in energy state E_2, and its decay path is to E_1, but, before it has a chance to spontaneously decay, a photon happens to pass by whose energy is approximately E_2-E_1, there is a probability that the passing photon will cause the electron to decay in such a manner that a photon is emitted at exactly the same wavelength, in exactly the same direction, and with exactly the same phase as the passing photon. This process is called "stimulated emission." Absorption, spontaneous emission, and stimulated emission are illustrated in *Fig 221.a)*. Now consider the group of atoms shown in figure *Fig 2.2.b)*: all begin in exactly the same excited state, and most are effectively within the stimulation range of a passing photon. We also will assume that t is very long, and that the probability for stimulated emission is 100 percent. The incoming (stimulating) photon interacts with the first atom,

causing stimulated emission of a coherent photon; these two photons then interact with the next two atoms in line, and the result is four coherent photons, on down the line. At the end of the process, we will have eleven coherent photons, all with identical phases and all traveling in the same direction. In other words, the initial photon has been "amplified" by a factor of eleven. Note that the energy to put these atoms in excited states is provided externally by some energy source which is usually referred to as the "pump" source.

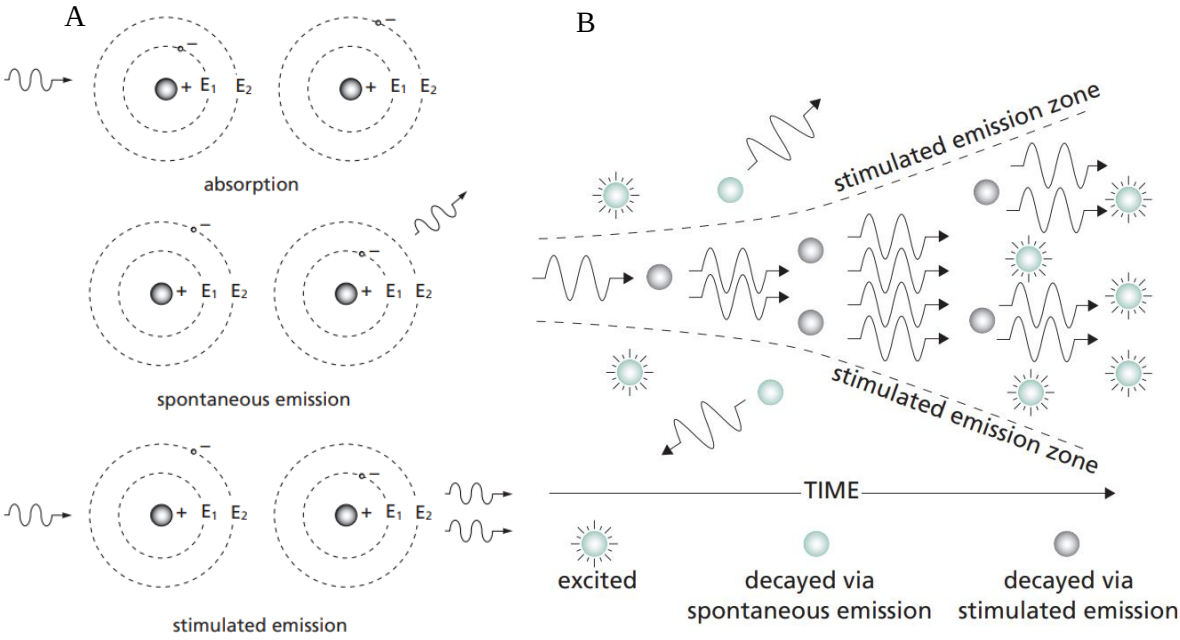

***Fig 2.2** a) Spontaneous and stimulated emissions b) Amplification by stimulated emission*

Of course, in any real population of atoms, the probability for stimulated emission is quite small. Furthermore, not all of the atoms are usually in an excited state; in fact, the opposite is true. Boltzmann's principle, a fundamental law of thermodynamics, states that, when a collection of atoms is at thermal equilibrium, the relative population of any two energy levels is given by

$$\frac{N_2}{N_1} = \exp\left(-\frac{E_2 - E_1}{kT}\right)$$

where N_2 and N_1 are the populations of the upper and lower energy states, respectively, T is the equilibrium temperature, and k is Boltzmann's constant. Substituting $h\nu$ for E_2-E_1 yields

$$\Delta N \equiv N_1 - N_2 = \left(1 - e^{-h\nu/kT}\right) N_1.$$

For a normal population of atoms, there will always be more atoms in the lower energy levels than in the upper ones. Since the probability for an individual atom to absorb a photon is the same as the probability for an excited atom to emit a photon via stimulated emission, the collection of real atoms will be a net absorber, not a net emitter, and amplification will not be possible. Consequently, to make a laser, we have to create a "population inversion."

Components of the laser

A laser system generally requires three components for its generation. They are

- active medium
- pumping source
- an optical resonator

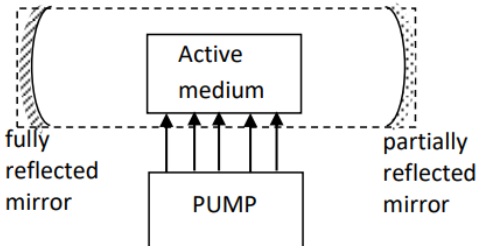

Active medium:

An active medium is one with energy levels having a population inversion between some levels and the laser action takes place here. It may be solid, liquid or gas. This medium determines the wavelength of the laser.

Pumping source:

The pump is an external energy source that supplies energy needed to transfer the laser medium into the state of population inversion. There are different types of pumping methods such as optical, electrical, chemical etc.

Optical Resonator (Resonant cavity):

It consists of a pair of parallel mirrors between which the active medium is kept. The mirrors could be either plane or curved. One of the mirrors is fully reflecting and the other is partially reflecting. Photons emitted during stimulated emission are shuttled between these two mirrors and as a result, more coherent laser beam is produced. Thus, it provides the feedback necessary to produce coherent stimulated emission.

Resonator and lasing action

The population inversion condition in itself is not enough for laser oscillations to occur. A large number of excited atoms decay spontaneously and each spontaneous photon can initiate in the active medium many other stimulated transitions. Photo states are characterized by a definite energy, momentum and polarization of photons. photons occupying the are indiscernible. They are discernible only when they are in different states. Since the spontaneous photons initiating the transitions are generally in different photon stales. they are useless from the point of view of coherent amplification. In order to obtain coherent radiation. it is necessary to restrict the number of photon states, The selectivity of photon states and the positive feedback that is necessary to offset the various types or losses, can be obtained by enclosing radiation in a resonator tuned to the frequency concerned.

Lasing action

Energy is applied to a medium raising electrons to an unstable energy level. These atoms spontaneously decay to a relatively long-lived, lower energy, metastable state. A population inversion is achieved when the majority of atoms have reached this metastable state. Lasing action occurs when an electron spontaneously returns to its ground state and produces a photon. it will stimulate the production of another photon of the same wavelength and resulting in a cascading effect. The highly reflective mirror and partially reflective mirror continue the reaction by directing photons back through the medium along the long axis of the

laser. The partially reflective mirror allows the transmission of a small amount of coherent radiation that we observe as the "beam". Laser radiation will continue as long as energy is applied to the lasing medium.

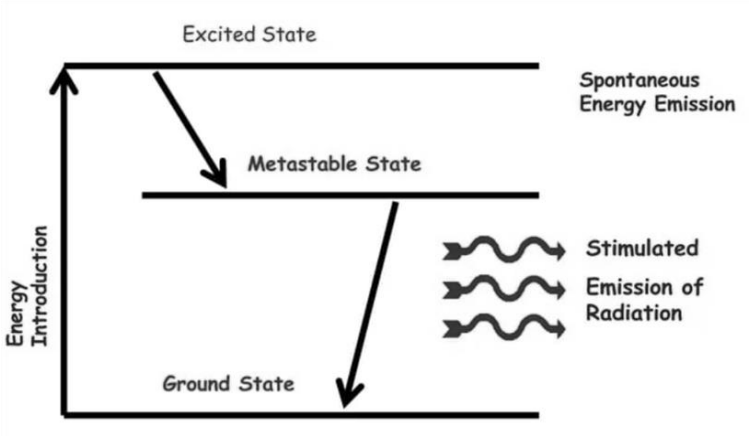

Fig 2.3 Lasing action diagram

Types of lasers and its applications

Lasers come in various types, each with its unique characteristics, wavelength, and applications. Here are some common types of lasers along with their applications:

Gas Lasers

Carbon Dioxide (Co_2) Lasers: Emit infrared light. Used in cutting, welding, engraving, and surgery.

Helium-Neon (He-Ne) Lasers: Emit red light. Commonly used in barcode scanners, alignment, and holography.

Solid-State Lasers

Nd: YAG Lasers (Neodymium-doped Yttrium Aluminum Garnet): Emit near-infrared light. Used in welding, drilling, cutting, and medical procedures like dermatology.

Ruby Lasers: Emit visible red light. Historically used in research and early medical applications.

Fiber Lasers: Use optical fibers as the gain medium. Widely used in material processing (cutting, welding), telecommunications, and medicine.

Diode-Pumped Solid-State Lasers (DPSSL): Use semiconductor diodes as pump sources. Applications include materials processing, telecommunications, and medical equipment.

Titanium-Sapphire Lasers: Emit in the near-infrared to visible range. Used in spectroscopy, biomedical research, and supercontinuum generation.

Semiconductor Lasers (also known as Diode Lasers)

Laser Diodes: Emit in various wavelengths from ultraviolet to infrared. Used in telecommunications, optical storage (CD, DVD), laser printing, and medical devices.

Vertical-Cavity Surface-Emitting Lasers (VCSELs): Emit low-power, circular beams. Used in data communication (fiber optics), laser printers, and computer mice.

Excimer Lasers: Emit in the ultraviolet range. Used in eye surgery (LASIK), semiconductor manufacturing, and microfabrication.

Chemical Lasers

Use a chemical reaction to produce laser light. Applications include military weaponry, industrial cutting, and research.

Free-Electron Lasers (FELs)

Emit across a wide range of wavelengths from infrared to X-rays. Used in research, medical imaging, and materials science.

Dye Lasers

Use organic dye solutions as the gain medium. Emit in the visible to near-infrared range. Applications include spectroscopy, medicine, and research.

Solid state lasers

Solid-state lasers are a class of lasers where the lasing medium is a solid material rather than a liquid or gas. They operate based on the principle of stimulated emission, where atoms or ions in the solid gain energy and emit photons when stimulated by an external energy source. The solid-state laser medium can be composed of various materials like crystals (e.g., ruby, Nd: YAG), glasses, or ceramics doped with atoms or ions that provide the necessary energy levels for lasing action.

One of the key advantages of solid-state lasers is their efficiency and reliability compared to other types of lasers. They can produce high-quality, coherent light with excellent beam characteristics, making them valuable in a wide range of applications including scientific research, medical procedures, materials processing, telecommunications, and defense systems.

Solid-state lasers offer versatility in terms of output wavelength, pulse duration, and power levels, depending on the specific design and doping elements used in the laser medium. Their compact size, robustness, and relatively low maintenance requirements have contributed to their widespread adoption in diverse industries

Ruby laser

The ruby laser was the first laser. It operates in a pulsed mode at 694.3 nm with an emission linewidth of 0.53 nm. The ruby laser rod consists of a sapphire crystal ($A1_2O_3$) with chromium ions (Cr^{3+}) doped in at a typical concentration of 0.05% by weight. At this concentration there are approximately 10^{25} Cr ions per cubic meter. The ruby laser is typically flashlamp-pumped with pulse durations ranging from a fraction of a millisecond to a few milliseconds. The laser can also be Q-switched. The pumping absorption bands occur at 400 nm and 550 nm with an approximate bandwidth of 50 nm at each wavelength, and thus they match very well with the pumping spectrum of xenon flashlamps. The laser is a three-level system. Therefore, has a much higher pumping threshold than such four-level laser systems as the Nd: YAG laser. However, the ruby laser does have an exceptionally long upper laser level

lifetime of 3 ms, which gives it an unusually high energy-storage capability. Pulse energies of up to 100 J are possible, although the pulse repetition rate is low (1-2 pulses per second) and hence limits the average power. This limitation is due to the excess heat produced by the high pumping flux required to produce laser output. Relaxation oscillations often occur in this laser. The ruby crystal is hard and durable, has good thermal conductivity, and is chemically stable. Ruby laser crystals, from which laser rods are cut, can be grown with very high optical quality.

Laser Structure

Ruby laser rods can be grown in diameters of up to 25 mm and rod lengths of up to 0.2 m. The rods are generally placed in a double elliptical cavity with two linear flashlamps for the pumping source, as indicated in Fig 2.4.

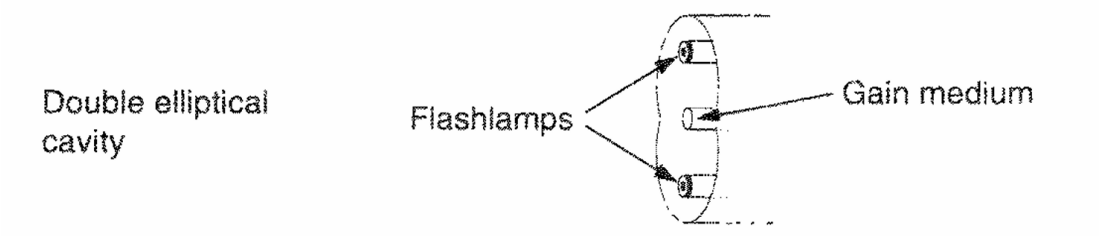

Fig 2.4 Two linear flashlamps

The mirrors are typically external to the rod and are usually flat or slightly concave. Thermal lensing of the rod itself during the pumping cycle is compensated by the slightly curved mirrors. The rear mirror typically has high reflectivity and the output mirror is partially transmitting. The laser can also be operated in an oscillator-amplifier configuration. In this case the beam that is input to the amplifier should be at or above the saturation intensity in order to extract energy efficiently from the amplifier. Because of the high pumping flux required for this laser, water is generally flowed in the region of the pumping cavity to remove excess heat from the laser rod. Since the water is transparent in the wavelength region of the pumping bands, it has little effect upon reducing the pumping flux from the flashlamp before it is absorbed by the rod. A diagram of the first ruby laser is shown in Fig 2.5.

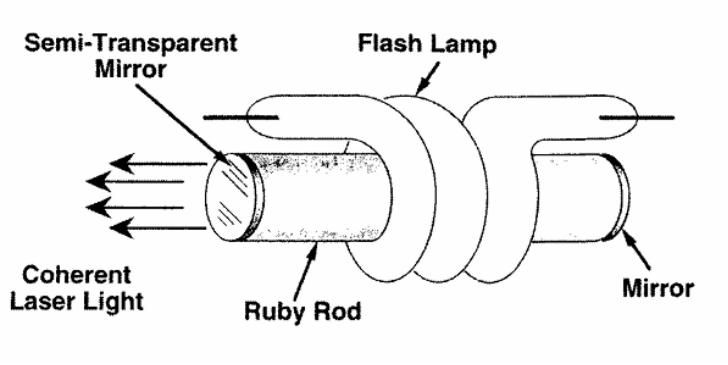

Fig 2.5 The first ruby laser

Excitation Mechanism

The energy-level diagram for ruby shown in Fig 2.6 involves a $^4A_2$ ground state with a statistical weight of g = 4, two excitation bands of $^4F_2$ accessed by pumping with green light and $^4F_1$ accessed with blue light. These two energy bands rapidly decay in a time of the order

of 0.1 μs to two ^{2}E levels. The upper of these two levels is the 2 level with a statistical weight of g = 2 and the lower level, the $\bar{E}$ level with g = 2, serves as the upper laser level. The transition from the $\bar{E}$ level to the $^4A_2$ level is the laser transition at 694.3 nm. We have stated that the lifetimes of the ^{4}F energy bands are extremely short. Thus, when excitation is applied to a ruby laser rod, most of the population resides either in one of the ^{2}E levels or in the $^4A_2$ ground state. The optical transitions $\bar{E} \rightarrow {}^4A_2$ and $2\bar{A} \rightarrow {}^4A_2$ are referred to as the R_1 and R_2 lines, occurring at wavelengths of 694.3 nm and 692.9 nm (respectively). In thermal equilibrium, the populations of these two levels are determined by a Boltzmann distribution. Hence, if the crystal is maintained at room temperature during the pumping process, there would generally be approximately 15% more population in the $\bar{E}$ level than in the $2\bar{A}$ level at any given time.

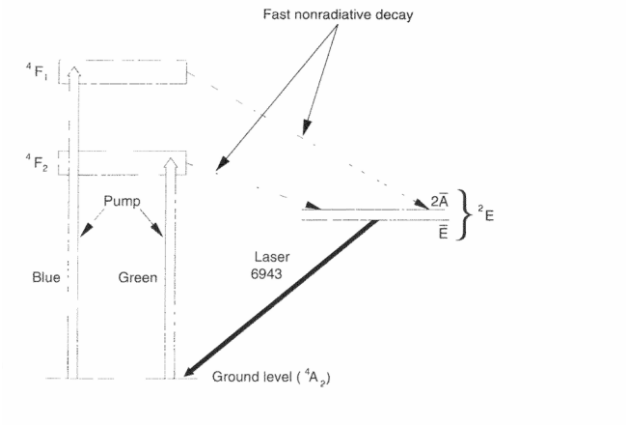

Fig 2.6 Energy-level diagram of ruby laser

Nd: YAG laser

The Nd ion when doped into a solid-state host crystal produces the strongest emission at a wavelength just beyond μm. The two host materials most commonly used for this laser ion are yttrium aluminum garnate (YAG) and glass. When doped in YAG ($Y_3A_{15}O_{12}$), the Nd: YAG crystal produces laser output primarily at 1.064 μm; when doped in glass, the Nd: glass medium lases at wavelengths ranging from 1.054 to 1.062 μm, depending upon the type of glass used. Nd also lases at 0.94 μm and at 1.32 μm from the same upper laser level as the 1.064-μm transition, although these transitions have lower gain. The Nd laser incorporates a four-level system and consequently has a much lower pumping threshold than that of the ruby laser. The upper laser level lifetime is relatively long (230 μs for Nd: YAG and 320 μs for Nd: glass), so population can be accumulated over a relatively long duration during the pumping cycle when the laser is used either in the Q-switching mode or as an amplifier. The emission and gain linewidths are 0.45 nm for YAG and 28 nm for glass. In YAG, the laser transition is homogeneously broadened by thermally activated lattice vibrations. These lasers can be pumped either by flashlamps or by other lasers. Diode pumping is a relatively recent technique that has led to the development of much more compact Nd lasers, both at the fundamental wavelength of 1.06 μm and at the frequency-doubled wavelength of 0.53 μm. The Nd: YAG crystal has good optical quality and high thermal conductivity, making it possible to provide pulsed laser output at repetition rates of up to100 Hz. The crystal size is limited to lengths of approximately 0.1 m and diameters of 12 mm, thereby limiting the power and energy output capabilities of this laser. Doping concentrations for Nd: YAG crystals are typically of the order of 0.725% by weight, which corresponds to approximately 1.4 x 10^{26} atoms per cubic meter.

For Nd: glass laser gain media, very large size laser materials have been produced. Rods of up to 2 m long and 0.075 m in diameter and disks of up to 0.9 m in diameter and 0.05 m thick have been successfully demonstrated. The large-diameter disks have been used as amplifiers to obtain laser pulse energies of many kilojoules (see Figure 15-8). The drawback of Nd: glass laser materials is their relatively poor thermal conductivity, which restricts these lasers to relatively low pulse repetition rates. For example, a large Nd: glass laser system constructed at Lawrence Liver-more National Laboratories, the NOVA laser, produces output pulses of up to several kilojoules per pulse but can be pulsed at a repetition rate of only several pulses per day. If the large glass amplifiers are not allowed to cool down completely between pulses, thermal and optical distortion severely reduce the energy of the subsequent pulse, with the risk (due to self-focusing effects) of damaging the amplifiers.

Laser Structure

Neodymium-doped lasers range from small diode-pumped versions with outputs of a few milliwatts, doubled into the green, up to high average-power lasers with average powers of up to several kilowatts. The high average-power lasers use either oscillator amplifier combinations or slab lasers as described in Fig 2.7. The laser structure for Nd lasers can be categorized as follows: flashlamp-pumped Nd: YAG lasers, both cw and pulsed; diode-pumped Nd: YAG lasers; and large Nd: glass amplifiers.

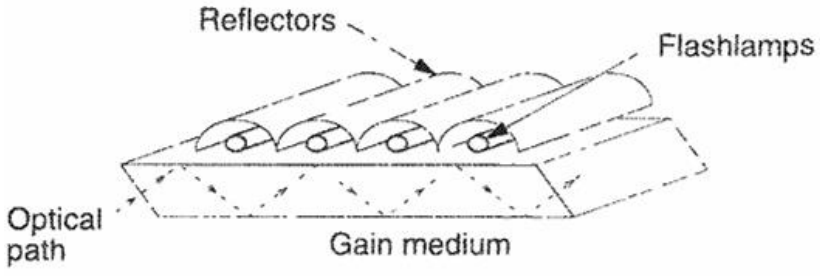

Fig 2.7 Slab laser amplifier

FLASHLAMP-PUMPED Q-SWITCHED Nd: YAG LASERS

One of the most useful types of Nd: YAG lasers is the flashlamp-pumped Q-switched oscillator amplifier system. The system includes a double elliptical pumping arrangement, consisting of two linear flashlamps and a 6-mm diameter, 0.1-m long Nd: YAG laser rod with antireflection coatings on both ends of the rod. This laser road assembly is installed inside an unstable resonator laser cavity along with a Pockels cell Q-switching device. The amplifier typically increases the oscillator output energy by up to a factor of 10.

FLASHLAMP-PUMPED cw Nd: YAG LASERS

This heading is really a misnomer, for two reasons. First, when a lamp is operated cw rather than pulsed, it is generally referred to as an "arc" lamp rather than a "flash" lamp. Second, although the laser gain medium is pumped by a cw arc lamp, the laser is actually not a true cw laser but instead is Q-switched at a high repetition rate, of the order of 20 kHz, to produce 200-300-ns pulses with an average power of as much as 15 W. This high average-power long-pulse laser differs from the laser described in the previous section, which is flashlamp pumped to produce high peak-power, Q-switched pulses of only 10-ns duration. The longer pulse duration

obtained from the arc lamp-pumped laser is used extensively for materials processing applications. This type of laser is also very effective for frequency doubling the 1.06 μm light to the green at 0.53 μm.

DIODE-PUMPED Nd: YAG LASERS

A generic version of a diode-pumped solid-state laser. A number of laser manufacturers are currently developing compact diode-pumped Nd: YAG lasers. The GaAs laser diode has the ideal pumping wavelength for the Nd^{3+} ion in the region of 0.8 μm. Many of the applications for a diode-pumped Nd: YAG laser are in the green portion of the spectrum, making it necessary to frequency-double the 1.06- μm laser output to 0.53 μm, a wavelength near the peak of the response of the human eye. The cavity arrangement of a diode-pumped, frequency-doubled Nd: YAG laser. This unique arrangement allows the operation of a two-mirror ring laser by taking advantage of the refraction of the laser beam at the output of the Nd: YAG laser rod at the Brewster angle to direct the beam toward the output mirror. The doubling crystal could be mounted intracavity for high conversion efficiency. This laser produces single-frequency output of greater than 10 mw and a linewidth of less than 2 MHz with a consequently large longitudinal coherence length of greater than 150 m.

Nd: GLASS AMPLIFIERS

Nd: glass laser materials are primarily used as amplifiers for very large pulsed lasers. They have played a major role in the development of the laser fusion program. Lawrence Livermore National Laboratories developed the NOVA laser, consisting of eight separate glass amplifier beamlines arranged in parallel and all fed by a single oscillator. Each beamline consists of approximately 20 amplifier stages, each using 3-5 flashlamp-pumped glass amplifier slabs arranged. Each beamline has an input energy per pulse of approximately 100 nJ from the common oscillator and a final output energy of approximately 10 kJ over a pulse duration of 1—2 ns. Thus, a total gain of 10^{11} is achieved in each amplifier beamline, producing a combined energy from the eight beamlines of 80 kJ and a peak power of up to 8 x 1013 W! An even larger laser, referred to as the National Ignition Facility (NIF), would consist of 192 beamlines or arms, each consisting of a series of approximately 20 Nd: glass amplifier stages. The glass in these amplifiers would be Nd-doped phosphate glass. Each slab in the amplifiers would have a gain coefficient similar to that of the slabs in the NOVA laser, 0.55% per millimeter, yielding a total gain similar to that of the NOVA laser system. The final output stage of each beamline would consist of large glass slabs with an effective aperture nearly 0.4 m square, pumped by large-bore xenon flashlamps. The parts would be modular to simplify servicing of the laser. Each beamline would produce an output energy of 15 kJ in a pulse duration of 3.5 ns for a total energy of nearly 3 M J!

Excitation Mechanism

The Nd laser energy levels doped in both YAG and glass were shown in Fig 2.8 and 2.9. The $^4F_{3/2}$ upper laser level is split into two components, referred to as R_1 and R_2. The R_2 component is the upper laser level and is approximately 0.011 eV above the R_1 level. Because these levels are closely coupled, their populations generally exist in a Boltzmann distribution (eqn. 6.11) and hence at room temperature only about 40% of their combined population is in the upper laser level. Thus, as laser action occurs and stimulated emission depletes the upper laser level, it is rapidly replenished by the population in the R_1 level until both are depleted. As

seen from the figures just referred to, there is a broad range of pumping wavelengths in the Nd: YAG system over the region from 0.3 to 0.9 um. This range includes two strong bands, at 0.75 um and 0.81 um, that make these lasers attractive for pumping with efficient diode lasers. The lower laser level is 0.26 eV above the ground state. As a result, there is essentially no significant thermal population in the lower laser level at room temperature and hence the lower laser level decays extremely rapidly by thermalizing collisions. This makes the pumping threshold very low. Thus, excitation can be achieved with broadband xenon flashlamps as well as with other lasers, in particular the Gas diode laser that can be matched with the 0.81 μm pump band.

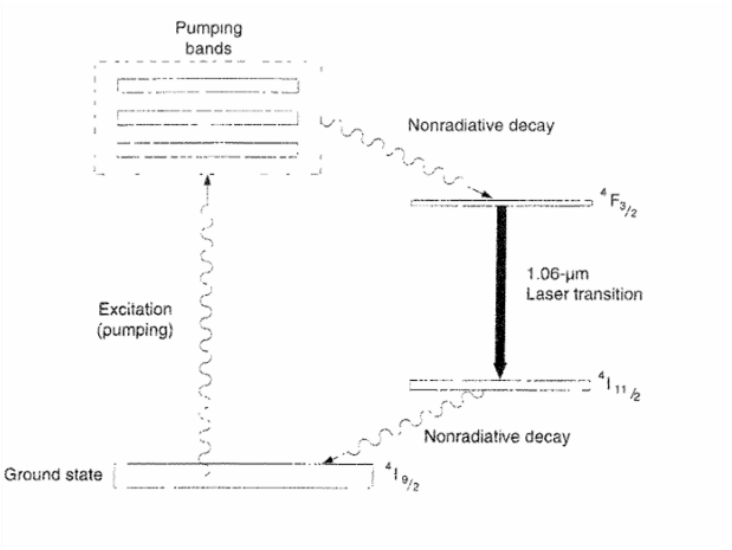

Fig 2.8 Energy levels of the Nd: YAG laser crystal

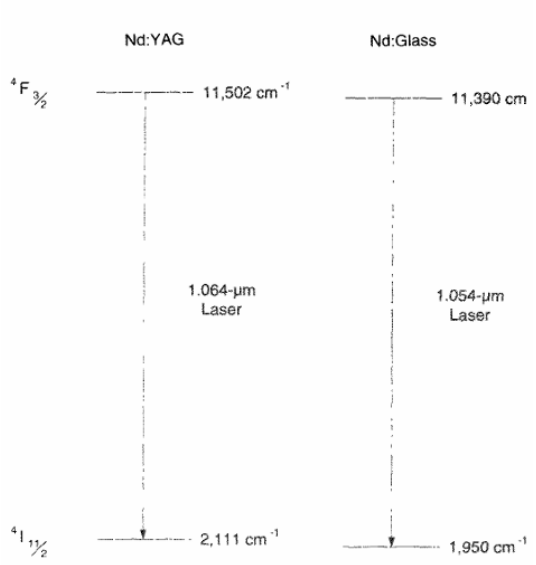

Fig 2.9 Comparison of energy levels of the laser transition for Nd doped in YAG and glass

Gas lasers

Gas lasers are a fascinating class of lasers that utilize a gas medium to produce coherent light. They operate on the principle of stimulated emission, where atoms or molecules in the gas are excited to higher energy states and then stimulated to emit photons as they return to lower energy states. The gas medium can vary, including helium, neon, carbon dioxide, and argon, among others, each contributing unique properties to the laser output.

Gas lasers offer several advantages, including high power output, good beam quality, and tunability across a wide range of wavelengths. They find applications in various fields such as research, medicine, industry, and telecommunications. Common types of gas lasers include helium-neon (HeNe) lasers, carbon dioxide (CO_2) lasers, argon-ion lasers, and excimer lasers.

HeNe lasers, for example, are widely used in scientific experiments, barcode scanners, and alignment applications due to their stable output and visible red light. CO_2 lasers, on the other hand, are prized for their high-power output and are extensively used in industrial cutting, welding, and engraving processes. Argon-ion lasers find applications in microscopy, spectroscopy, and holography, owing to their multiple visible wavelengths.

He-Ne laser

The He Ne laser consists of a mixture of He and Ne in a ratio of about 10:1, placed inside a long narrow discharge tube (see Fig 2.10). The pressure inside the tube is about 1 Torr. * The gas system is enclosed between a pair of plane mirrors or a pair of concave mirrors so that a resonator system is formed. One of the mirrors is of very high reflectivity while the other is partially transparent so that energy may be coupled out of the system.

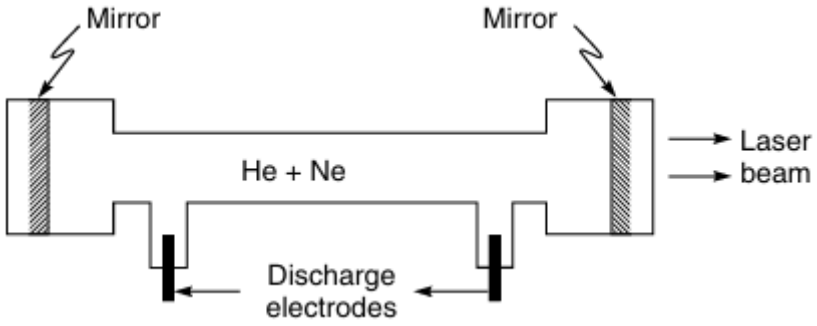

Fig 2.10 The helium—neon laser

The first few energy levels of He and Ne atoms are shown in Fig 2.11. When an electric discharge is passed through the gas, the electrons traveling down the tube collide with the He atoms and excite them (from the ground state F_1 the levels marked F_2 and F_3) to. These levels are metastable, i.e., He atoms excited to these states stay in these levels for a sufficiently long time before losing energy through collisions.

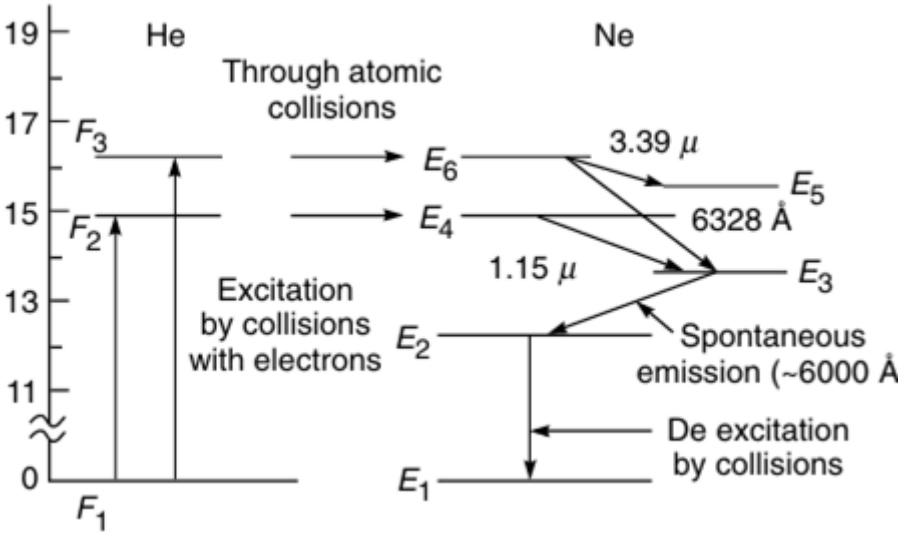

Fig 2.11 Relevant energy levels of helium and neon

Through these collisions, the Ne atoms are excited to the levels marked E_4 and E_6 which have nearly the same energy as the levels F_2 and F_3 of He. Thus, when the atoms in levels F_2 and F_3 collide with unexcited Ne atoms, they raise them to the levels E_4 and E_6 respectively. Thus, we have the following two step process:

(a) Helium atom in the ground state F1 + collision with electron

→Helium atom in the excited state (F_2 or F_3) + electron with lesser kinetic energy.

(b) The excited states of He (F_2 or F_3) are metastable* they would not readily lose energy through spontaneous emissions (the radioactive life time of these excited states would be about one hour). How ever, they can readily lose energy through collisions with Ne atoms:

He atom in the excited state F_3 + Ne atom in the ground state

→He atom in the ground state + Ne atom in the excited state E_6.

Similarly,

He atom in the excited state F_2 + Ne atom in the ground state.

→He atom in the ground state + Ne atom in the excited state E_4.

This results in a sizeable population of the levels E_4 and E_6. The population in these levels happens to be much more than those in the lower levels E_3 and E_5. Thus, a state of population inversion is achieved and any spontaneously emitted photon can trigger laser action in any of the three transitions shown in Fig 2.11. The Ne atoms then drop down from the lower laser levels to the level E_2 through spontaneous emission. From the level E_2 the Ne atoms are brought back to the ground state through collision with the walls. The transition from E_6 to E_5, E4 to E_3 and E_6 to E_3 result in the emission of radiation having wavelengths 3.39 m, 1.15 m and 6328 Å, respectively. It may be noted that the laser transitions corresponding to 3.39 m and 1.15 m are not in the visible region. The 6328 Å transition corresponds to the well-known red light of the HeNe laser. A proper se lection of different frequencies may be made by choosing end mirrors having high reflectivity over only the required wavelength range. The pressures of the

two gases must be so chosen that the condition of population inversion is not quenched. Thus, the conditions must be such that there is an efficient transfer of energy from He to Ne atoms. Also, since the level marked E_2 is metastable, electrons colliding with atoms in level E_2 may excite them to level E_3, thus de creasing the population inversion. The tube containing the gaseous mixture is also made narrow so that He atoms in level E_2 can get de-excited by collision with the walls of the tube. Referring to Fig 2.11, it may be mentioned that actually there are a large number of levels grouped around E_2, E_3, E_4, E_5 and E_6. Only those levels are shown in the figure which correspond to the important laser transitions. ** Gas lasers are, in general, found to emit light, which is more directional and more monochromatic. This is because of the absence of such effects as crystalline imperfection, thermal distortion and scattering, which are present in solid state lasers. Gas lasers are capable of operating continuously without need for cooling

CO_2 laser

The carbon dioxide laser is one of the most powerful and efficient lasers available. It operates in the middle infrared on rotational vibrational transitions in the 10.6-μm and 9.4-μm wavelength regions. Both pulsed and cw laser output occurs in several different types of gas discharge configurations in a mixture of carbon dioxide, nitrogen, and helium gases, typically with a CO_2: N_2 ratio of about 0.8: 1 and with somewhat more helium than N_2. These lasers have produced cw powers of greater than 100 kW and pulsed energies of as much as 10 kJ. The gain occurs on a range of rotational—vibrational transitions that are dominated by either Doppler broadening or pressure broadening, depending upon the gas pressure. The lasers range from small cw waveguide-type systems of the order of 0.35 m long to much larger pulsed laser amplifiers that a person could walk through designed for laser fusion. One of the most useful CO_2 lasers for materials application is a cw version with a cavity length of 1-2 m producing one or more kilowatts of power. Another laser of this class is the CO laser, which emits at approximately half the wavelength of the CO_2 laser in the 5-6μm wavelength region.

Laser Structure

There are a number of different types of laser structures used for the CO_2 laser. These structures are depicted in Fig 2.12 and can be summarized as follows.

Longitudinally excited lasers

These lasers are operated as conventional gas discharge lasers in the form of long, narrow, cylindrically shaped glass enclosures with electrodes at opposite ends from which the discharge excitation current is introduced, as seen in Fig 2.12 (a). These lasers can be either pulsed or cw and can have lengths of up to several meters. In some versions the discharge enclosure is sealed off, requiring periodic replacement of the tube because the gases eventually

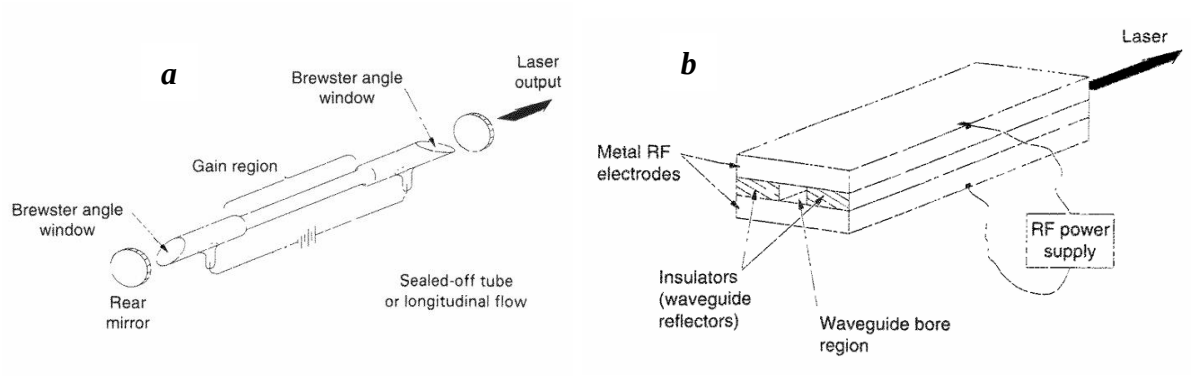

Fig 2.12 (a) Longitudinal discharge CO_2 laser (b) Waveguide CO_2 laser

degrade owing to breakdown of the CO_2, which produces oxygen that can corrode the electrodes. In other versions, the gas is flowed through the tube longitudinally and can be recirculated to conserve the gases. Discharge currents of hundreds of milliamps and tube-bore diameters of several centimeters are common for this type of laser. A water coolant jacket usually surrounds the discharge region.

Excitation Mechanism

Detailed energy-level diagrams of the CO_2 laser were shown in Fig 2.13 and 2.14. Those figures showed the close energy coincidence between the N_2 v= 1 vibrational level and the (0, 0, 1) vibrational level (upper laser level) of CO_2. Although laser action can be produced in pure CO_2 gas, such action is very inefficient with low gain. When N_2 is added to the discharge this laser becomes one of the more efficient ones, with "wall plug" efficiencies as high as 30%. The nitrogen v= 1 vibrational level is efficiently excited but is metastable to radiative decay. It thus accumulates population, which is then collisionally transferred to the CO_2 (0, 0, I) vibrational level. The upper laser level is the Σ_u level involving the asymmetric stretch mode of vibration, whereas the lower laser level is the (l, 0, 0) symmetric stretch Σ_g level. The radiative decay rate from the lower laser level is approximately 20 times faster than the decay from the upper laser level, which establishes the population inversion.

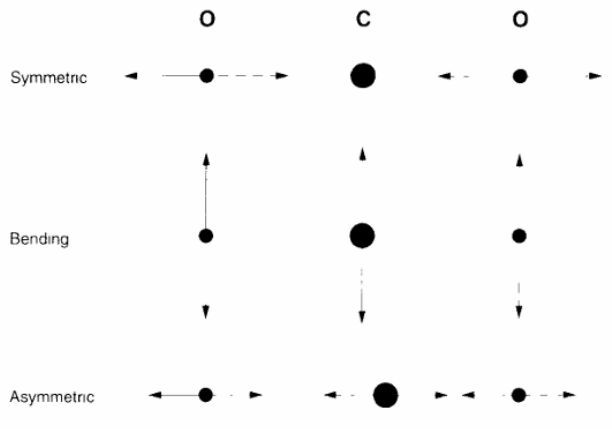

Fig 2.13 Vibrational modes Of the CO_2 molecule

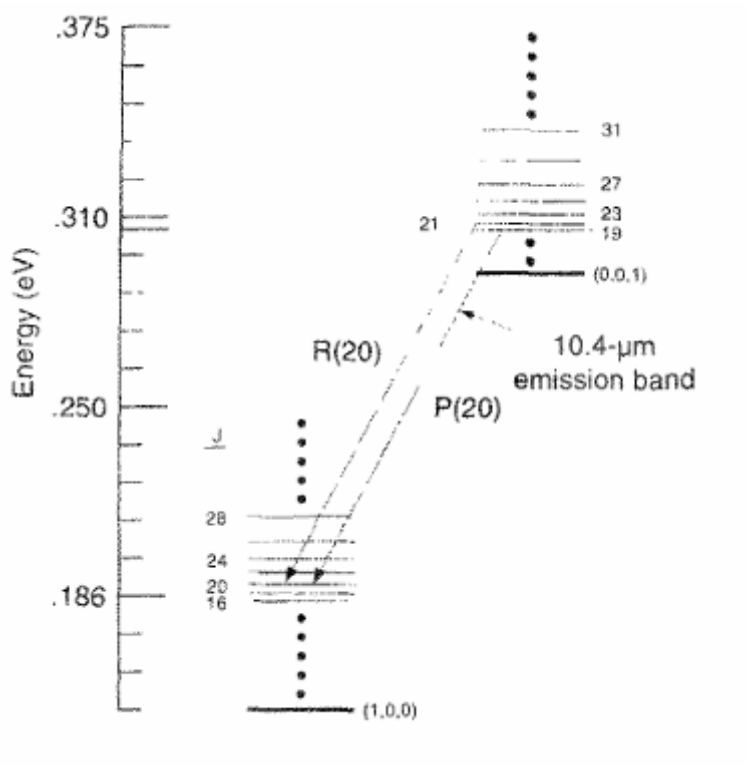

Fig 2.14 Two specific P and R-branch laser transitions of the CO_2 molecule

Chemical lasers

Chemical lasers are lasers in which the pumping energy is obtained from a chemical reaction. These lasers typically operate on molecular transitions, although there is one atomic chemical laser operating in atomic iodine. Most chemical lasers operate in the near - to middle-infrared portion of the spectrum. The most well-known chemical lasers are those operating on vibrational transitions of hydrogen fluoride and deuterium fluoride. Chemical lasers have been developed primarily for military and space applications, where pumping power in the form of electrical energy might not be available. Chemical lasers have been developed that emit powers up to several megawatts for antimissile defense. The hydrogen fluoride laser emits in the wavelength range of 2.6-3.3 μm, a region of high absorption within the atmosphere. By using deuterium instead of hydrogen, the laser wavelength range is shifted to 3.5-4.2 μm, a region where the atmospheric absorption is low. Other chemical lasers include the HBr laser operating at 4.0-4.7 μm, the CO laser at 4.9-5.8 μm, and the CO_2 laser at 10.0-11.0 μm.

Laser Structure

Chemical lasers are typically devices in which the chemical vapor is mixed and then flowed through the gain region in a direction transverse to the laser beam axis. Toxic and combustible chemicals are generated in such lasers, and the residual gases must be either neutralized or collected for later disposal. Special nozzles are used to generate the appropriate flow conditions within the gain region in order to maximize efficiency of these lasers.

Excitation Mechanism

Chemical lasers are generally initiated by a chemical reaction within which the excited laser species is produced. The HF and DF lasers are produced by mixing hydrogen with fluorine gas.

There are a few commercial HF/DF lasers that pro-vide the fluoride atoms by dissociating SF_6 within a gas discharge and then flowing those species into a reaction chamber with hydrogen. Oxygen can be added to at-tract the free sulfur left over within the discharge. The atomic iodine laser, which operates at a wavelength of 1.3 μm, is produced via the generation of excited molecular oxygen by reacting molecular chlorine with hydrogen peroxide. This long-lived excited molecular oxygen in turn transfers its energy to atomic iodine, producing excitation to the upper laser level.

HCl laser

A number of systems of this type have been made to operate, One of the members of this class of lasers is the hydrogen chloride laser. When atomic hydrogen and chlorine combine, a substantial amount of energy is released and hydrogen chloride is formed in the excited state

$$H + Cl_2 \rightarrow HCl^* + Cl$$

HCl laser have shown that the reaction of atomic hydrogen with chlorine at low pressure 0.02 Torr, leads to high population in the upper vibrational levels, especially v = 3 and produces a population inversion. This gives laser emission on an HCl transition at= 3.77 μm. Thus, a general feature of the halogen-hydrogen reaction seems to be that a large part of the energy released by the chemical reaction is left as vibrational energy in the newly formed halogen-hydride molecules and in the low-pressure condition leads to laser action. This is, no doubt, a true chemical reaction; but, unfortunately, cannot yet be operated with purely chemical energy input. The only way to create the necessary free H atoms for this reaction is to dissociate the molecules in an H_2-Cl_2 mixture with a flash from a flash lamp(photodissociation) or dissociation by electron impingement. The latter technique is more frequently used as it starts the reaction in a very short time of the order of 10^{-8} to 10^{-7}s. The electrical input in this case considerably exceeds the laser output. High vibrational excitation leading to population inversion in certain rotational levels of the vibrational states v = 1 and v = 2, was also obtained in the flash-initiated reaction between hydrogen and chlorine at pressures between 3 and 10 Torr.

Semiconductor laser

When a light beam with photons whose energy is slightly higher than the bandgap energy, is passed through a semiconductor. there is a probability that an electron at the-top of the valence band absorbs a photon and move to the conduction band. There is an equal probability that an electron already present at the bottom of the conduction band is persuaded by the incident photon to move to the valence band, where it recombines with a hole and in the process releases a photon in the same state as that of the incident photon, thus amplifying the radiation. In order that the process of stimulated emission dominates over that of absorption, it is necessary to create a population inversion in the semiconductor. That is, the concentration of electrons at the bottom of the conduction band must be higher than that of holes at the top of valence band. Such a population inversion can be obtained by optical pumping or by pumping with an electron beam with fast moving electrons (~100 kV). This latter technique is used in cadmium sulphide lasers. The major impediment in this method is that a substantial part of the electron beam energy is lost in heating the semiconductor chip. This spoils the degree of inversion as the electrons in the conduction band are lifted to the higher level, reducing their number at the bottom of the band and also moving electrons at the top of the valence band. Cooling, therefore, is essential for such intrinsic semiconductor lasers. Cadmium sulphide laser is found to operate successfully at liquid helium temperature 4.2 K at $\lambda = 0.49\mu m$.

UNIT – III
FIBEROPTICS

Introduction

Optics is today responsible for many revolutions in science and technology. This has been primarily brought about by the invention of the laser in 1960 and subsequent development in realizing extremely wide variety of lasers. One of the most important applications of lasers with its direct impact on our lives has been in communications. Use of electromagnetic waves in communication is quite old and the development of the laser gave communication engineers with a source of electromagnetic waves with extremely high frequency compared to microwaves and millimeter waves. The development of low loss optical fibers and also EDFAs (Erbium Doped Fiber Amplifiers) led to phenomenal growth in fiber optic communication systems. Today more than 10 terabits of information can be transmitted per second through one hair thin optical fiber; this amount of information is equivalent to simultaneous transmission of about 150 million telephone calls - this is certainly one of the very important technological achievements of the 20th century. We may also mention that in 1961, within one year of the demonstration of the first ever laser by Theodore Maiman, Elias Snitzer fabricated the first fiber laser which is now finding extremely important applications in many diverse areas from defense to sensor physics.

Total internal reflection

At the heart of an optical communication system is the optical fiber that acts as the transmission channel carrying the light beam loaded with information; and as mentioned earlier, the guidance of the light beam (through the optical fiber) takes place because of the phenomenon of total internal reflection (often abbreviated as TIR). Now, if a ray is incident at the interface of a rarer medium ($n_2 < n_1$) then the ray will bend away from the normal [see Fig 3.1 (b)]. The angle of incidence, for which the angle of refraction is 90°, is known as the critical angle and is denoted by ϕ_C. Thus, when

$$\boldsymbol{\phi_1 = \phi_C = sin^{-1}\left(\frac{n_2}{n_1}\right)}$$

the angle of refraction $\phi_2 = 90^0$. When the angle of incidence exceeds the critical angle (i.e., when $\phi_1 > \phi_c$), there is no re fracted ray and we have what is known as total internal reflection see Fig 3.1 (b). We may mention here that for $\phi_1 > \phi_c$, energy does penetrate into the rarer medium resulting in what is known as an evanescent wave; however, the reflection coefficient is unity.

Fig 3.1 (a) For a ray incident on a rarer medium (n2 < n1), the angle of refraction is greater than the angle of incidence, (b) if the angle of incidence is greater than critical angle, it will undergo total internal reflection.

The optical fiber

Optical fiber shown in Fig 3.2, which consists of a (cylindrical) central dielectric core cladded by a material of slightly lower refractive index. The corresponding refractive index distribution (in the transverse direction) is given by

$$\left.\begin{aligned} n &= n_1 \quad 0 < r < a \\ &= n_2 \quad r > a \end{aligned}\right\}$$

where n1 and n_2 (< n1) represent respectively the refractive indices of core and cladding and a represents the radius of the core. We define a parameter Δ through the following equations:

$$\Delta \equiv \frac{n_1^2 - n_2^2}{2n_1^2} \quad \text{.....3.1}$$

When $n_1 \approx n_2$ i.e., when $\Delta << 1$

$$\Delta = \frac{n_1 - n_2}{n_1}\frac{n_1 + n_2}{2n_1} \approx \frac{n_1 - n_2}{n_2} \approx \frac{n_1 - n_2}{n_1} \quad \text{.....3.2}$$

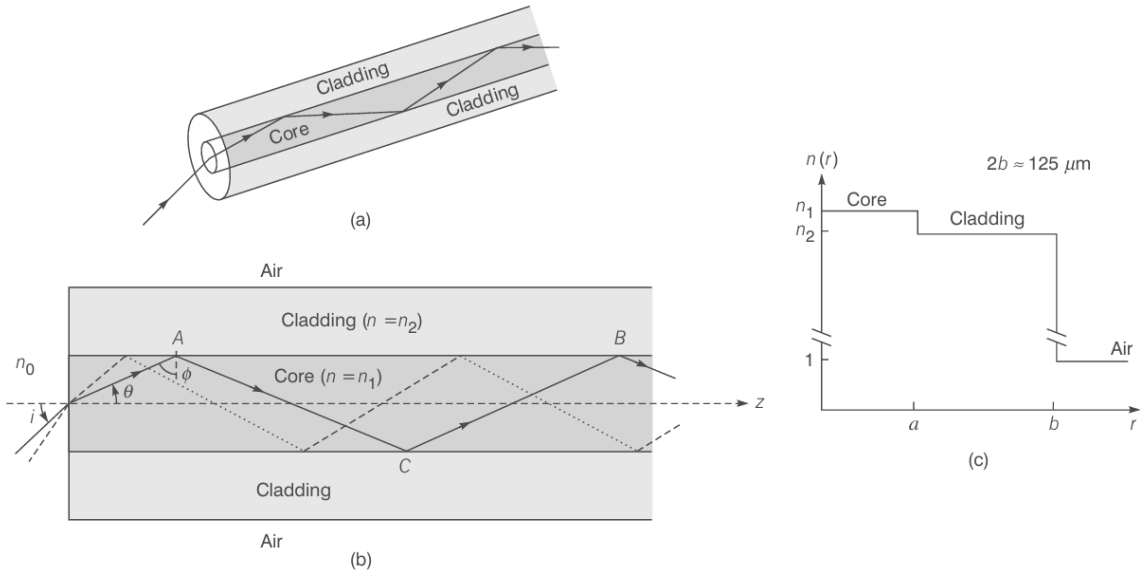

Fig 3.2 (a) A glass fiber consists of a cylindrical central core cladded by a material of slightly lower refractive index. (b) Light rays incident on the core-cladding interface at an angle greater than the critical angle are trapped inside the core of the fiber. (c) Refractive index distribution for a step-index fiber. The diameter of the cladding is almost always 125 μm. For multimode fibers, the core diameters are usually in the range of 25-50 μm. For single-mode fibers, the core diameters are usually between 5 and 10 μm

For a typical (multimoded) fiber, a ≈ 25 μm, n_2 ≈ 1.45 (pure silica) and Δ ≈ 0.01 giving a core index of n_1 ≈1.465. The cladding is usually pure silica while the core is usually silica doped with germanium; doping by germanium results in an increase of refractive index. Now, for a

ray entering the fiber, if the angle of incidence (at the core-cladding interface) is greater than the critical angle ϕ_c, then the ray will undergo TIR at that interface. Thus, for TIR to occur at the core-cladding interface.

$$\phi > \phi_c = \sin^{-1}\left(\frac{n_2}{n_1}\right)$$

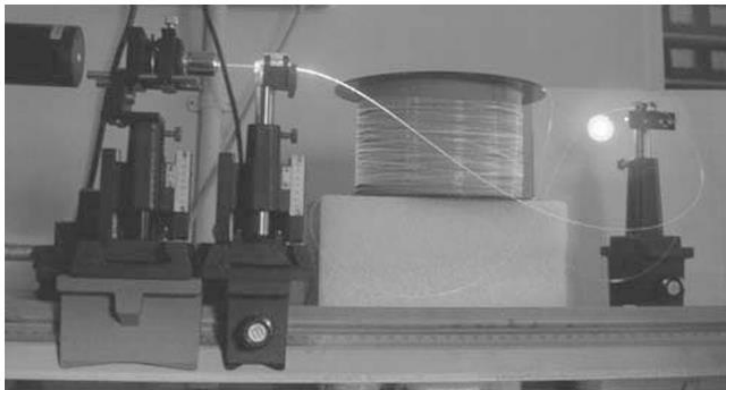

Fig 3.3 A step index multimode fiber illuminated by HeNe laser

Further, because of the cylindrical symmetry in the fiber structure, the ray will suffer TIR at the lower interface also and therefore get guided through the core by repeated total internal reflections. Even for a bent fiber, light guidance can occur through multiple total internal reflections. Fig 3.3 shows the actual guidance of a light beam as it propagates through a long optical fiber; in the photograph, the light emerging from the side of the fiber is mainly due to Rayleigh scattering, the same phenomenon that is responsible for the blue color of the sky and the red color of the rising or the setting sun (see Sec. 7.6) The necessity of a cladded fiber (Fig 3.2) rather than a bare fiber i.e., without a cladding, was felt because of the fact that for transmission of light from one place to another, the fiber must be supported, and supporting structures may consider ably distort the fiber thereby affecting the guidance of the light wave. This can be avoided by choosing a sufficiently thick cladding.

Glass fibers

In telecommunications and also in sensors, one always uses glass fibers. Why glass fibers? Glass is a remarkable material which has been in use in 'pure' form for at least 9000 years. The compositions remained relatively unchanged for millennia and its uses have been widespread. The three most important properties of glass which makes it of unprecedented value are:

- First, there is a wide range of accessible temperatures where its viscosity is variable and can be well controlled unlike most materials, like water and metals which remain liquid until they are cooled down to their freezing temperatures and then suddenly become solid. Glass, on the other hand, does not solidify at a discrete freezing temperature but gradually becomes stiffer and stiffer and eventually becoming hard. In the transition region, it can be easily drawn into a thin fiber.
- The second most important property is that highly pure silica is characterized with extremely low-loss; i.e., it is highly transparent. Today in most commercially available silica fibers 96% of the power gets transmitted after propagating through 1 km of optical fiber. This in deed represents a truly remarkable achievement.

- The third most remarkable property is the intrinsic strength of glass. Its strength is about 2000,000 lb/in^2 so that a glass fiber of the type used in the telephone network and having a diameter (125 m) of twice the thickness of a human hair, can support a load of 40 lb.

The coherent bundle

If a large number of fibers are put together, it forms what is known as a bundle. If the fibers are not aligned, i.e. they are all jumbled up, the bundle is said to form an incoherent bundle. However, if the fibers are aligned properly, i.e., if the relative positions of the fibers in the input and output ends are the same, the bundle is said to form a coherent bundle. Now, if a particular fiber is illuminated at one of its ends, then there will be a bright spot at the other end of the same fiber; thus, a coherent bundle will transmit the image from one end to another (see Fig 3.4)

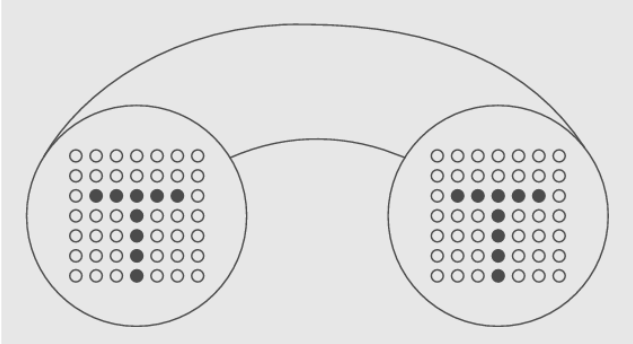

Fig 3.4 A bundle of aligned fibers.

In an incoherent bundle the output image will be scrambled. Incoherent bundles are used in illumination such as in traffic lights or road signs. They can also be used as cold light sources by removing the heat radiation using a filter at the input to the fiber bundle. The light emerging from the bundle is also free from UV radiation and is suitable for illumination of paintings etc. in museums

Perhaps the most important application of a coherent bundle is in a fiber-optic endoscope where it can be put in side a human body and the interior of the body can be viewed from outside, thus avoiding invasive surgery. In an endoscope; for illuminating the portion that is to be seen, the bundle is enclosed in a sheath of fibers which carry light from outside to the interior of the body. An incoherent bundle is often used to illuminate the area under investigation. And, a coherent bundle is used to transmit back the image. A typical fiber endoscope can have about 10000 fibers which would form a bundle of about 10 mm in diameter. Fiber endoscopes have revolutionized medical diagnosis and treatment.

The numerical aperture

Consider a ray (Fig 3.2) which is incident on the entrance aperture of the fiber making an angle i with the z-axis. Let the refracted ray make an angle with the axis. Assuming the outside medium to have a refractive index n_0 (which for most practical cases is unity), we get

$$\frac{\sin i}{\sin \theta} = \frac{n_1}{n_2}$$

Obviously if this ray has to suffer total internal reflection at the core-cladding interface,

$$\sin\phi(=\cos\theta) > \frac{n_2}{n_1} \qquad \ldots\ldots\ldots 3.3$$

Or

$$\sin\theta < \sqrt{1-\left(\frac{n_2}{n_1}\right)^2} \Rightarrow \sin i < \sqrt{\frac{\left(n_1^2 - n_2^2\right)}{n_0^2}}$$

In most cases, the outside medium is air, i.e.; no = 1, and therefore the maximum value of sin i for a ray to be guided is given by

$$\sin i_m = \begin{cases} \sqrt{n_1^2 - n_2^2} & \text{if } n_1^2 < n_2^2 + 1 \\ 1 & \text{if } n_1^2 < n_2^2 + 1 \end{cases}$$

Thus, if a cone of light is incident on one end of the fiber, it will be guided through it provided the semi-angle of the cone is less than im. The quantity sin im is known as the numerical aperture (NA) of the fiber and is a measure of the light gathering power of the fiber. In almost all practical situations, $n^2_1 < n^2_2+1$, and therefore one defines the numerical aperture of the fiber by the following equation:

$$\text{NA} = \sqrt{n_1^2 - n_2^2}$$

Attenuation in optical fibers

Attenuation and pulse dispersion represent the two most important characteristics of an optical fiber that determine the information carrying capacity of a fiber-optic communication system. Obviously, lower the attenuation (and similarly lower the dispersion), greater will be the required repeater spacing and therefore lower will be the cost of the communication system. Pulse dispersion will be discussed in the next section, while in this section, we will briefly discuss the various attenuation mechanisms in an optical fiber. The attenuation of an optical beam is usually measured in decibels (dB). If an input power P_{input} results in an output power P_{output}, then the loss in decibels is given by

$$\text{Loss (dB)} = 10\log_{10}\left(\frac{P_{\text{input}}}{P_{\text{output}}}\right)$$

Thus,

if the output power is the same as the input power, then the loss is = 0 dB;

if the output power is only one tenth of the input power, then the loss is = 10 dB;

if the output power is only one hundredth of the in put power, then the loss is = 20 dB; and if

the output power is only one thousandth of the input power, then the loss is = 30 dB; etc.

Also, in a typical fiber amplifier, a power amplification by a factor of 100 implies a power gain of 20 dB and a gain of 30 dB would imply a power amplification by a factor of 1000.

Single and multi-mode fibers

Solve Maxwell's equations for an optical waveguide then we obtain discrete modes which represent transverse field distributions that suffer only a phase change as they propagate through the waveguide along z. Each mode has a specific transverse field distribution and also a specific group velocity. Now, while studying the propagation of rays in an optical fiber [see Fig 3.2 (b)], we had assumed that all rays characterized by $\theta > \theta_c$ will be guided through the optical fiber. By solving Maxwells equations that each mode of the waveguide may be assumed to correspond to a discrete value of θ which would imply discrete ray paths; thus, qualitatively speaking, we may say that only discrete values of θ are possible. When the number of such discrete ray paths becomes very large, we have what is known as a multimode fiber and may assume the validity of geometrical optics

Pulse dispersion in multimode optical fibers

In digital communication systems, information to be sent is first coded in the form of pulses and then these pulses of light are transmitted from the transmitter to the receiver where the information is decoded. Larger the number of pulses that can be sent per unit time and still be resolvable at the receiver end, larger would be the transmission capacity of the system. A pulse of light sent into a fiber broadens in time as it propagates through the fiber; this phenomenon is known as pulse dispersion and occurs primarily because of the following mechanisms:

1. In multimode fibers, different rays take different times to propagate through a given length of the fiber. We will discuss this for a step index fiber and for a parabolic index fiber in this and the following sections. In the language of wave optics, this is known as intermodal dispersion because it arises due to different modes traveling with different velocities.
2. Any given light source emits over a range of wave lengths and, because of the intrinsic property of the material of the fiber, different wavelengths take different amounts of time to propagate along the same path. This is known as material dispersion and obviously, it is present in both single mode and multimode fibers.
3. On the other hand, in single-mode fibers since there is only mode, there is no intermodal dispersion; however, we have what is known as waveguide dispersion which is due to the geometry of the fiber. We will discuss single-mode fibers and waveguide dispersion. Obviously, waveguide dispersion is present in multimode fibers also but the effect is very small and can be neglected.

Ray dispersion in multimode step index fibers

We first consider ray paths in a step-index fiber as shown in Fig 3.2. As can be seen, rays making larger angles with the axis (those shown as dotted rays) have to traverse a longer optical path length and therefore take a longer time to reach the output end. We will now derive an expression for the intermodal dispersion for a step-index fiber. Referring back to Fig 3.2, for a ray making an angle with the axis, the distance AB is traversed in time

$$t_{AB} = \frac{AC + CB}{c/n_1} = \frac{AB/\cos\theta}{c/n_1} = \frac{n_1 AB}{c\cos\theta}$$

where c/n_1 represents the speed of light in a medium of refractive index n_1, being the speed of light in free space. Since the ray path will repeat itself, the time taken by a ray to traverse a length L of the fiber would be

$$t_L = \frac{n_1 L}{c\cos\theta}$$

The above expression shows that the time taken by a ray is a function of the angle θ made by the ray with the z-axis, which leads to pulse dispersion. If we assume that all rays lying between $\theta = 0$ and $\theta = \theta_c = \cos^{-1}(n_2/n_1)$ are present [see Eq. (3.3)], then the time taken by these extreme rays for a fiber of length L would be given by

$$t_{\min} = \frac{n_1 L}{c} \quad \text{corresponding to } \theta = 0$$

$$t_{\max} = \frac{n_1^2 L}{c n_2} \quad \text{corresponding to } \theta = \theta_c = \cos^{-1}(n_2/n_1)$$

Hence, if all the input rays were excited simultaneously, the rays would occupy a time interval at the output end of duration

$$\Delta\tau_i = t_{\max} - t_{\min} = \frac{n_1 L}{c}\left[\left(\frac{n_1}{n_2}\right) - 1\right]$$

$$\boxed{\Delta\tau_i \cong \frac{n_1 L}{c}\Delta \approx \frac{L}{2n_1 c}(\mathrm{NA})^2} \qquad \ldots\ldots\ldots 3.4$$

The above equation represents the intermodal dispersion in multimode SIF where Δ has been defined earlier [see Eqs. (3.1) and (3.2)] Assuming the validity of ray optics, is exact; however, in writing Eq. (3.4) we have assumed $\Delta << 1$, which is true for almost all commercially available silica fibers. The quantity $\Delta\tau_i$ represents the pulse dispersion due to different rays taking different times in propagating through the fiber which, in wave optics, is nothing but the intermodal dispersion and hence the subscript i. Note that the pulse dispersion is proportional to the square of NA. Thus, to have a smaller dispersion, one must have a smaller NA which of course reduces the acceptance angle and hence, the light gathering power. Now, if at the input end of the fiber, we have a pulse of width τ_1 then after propagating through a length L of the fiber, the pulse would have a width τ_2 given approximately by

$$\tau_2^2 = \tau_1^2 + \Delta\tau_i^2$$

Consequently, the pulse broadens as it propagates through the fiber (see Fig. 3.5). Hence, even though two pulses may be well resolved at the input end, because of the broadening of the pulses they may not be so at the output end

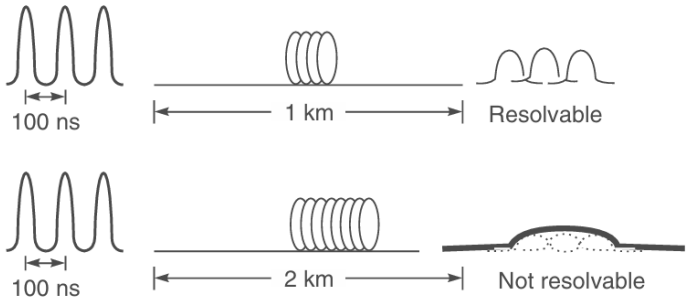

Fig 3.5 Pulses separated by 100 ns

Parabolic- index fibers

In a step-index fiber, such as that pictured in Fig.3.2, the refractive index of the core has a constant value. By contrast, in a parabolic-index fiber, (often abbreviated as PIF) the refractive index in the core decreases continuously (in a quadratic fashion) from a maximum value at the center of the core to a constant value at the core-cladding interface. (see Fig 3.6 corresponding to q = 2. The refractive index variation given by

$$n^2(r) = n_1^2\left[1 - 2\Delta\left(\frac{r}{a}\right)^2\right] \qquad 0 < r < a \quad \text{core}$$

$$= n_2^2 = n_1^2(1 - 2\Delta) \qquad r > a \qquad \text{cladding}$$

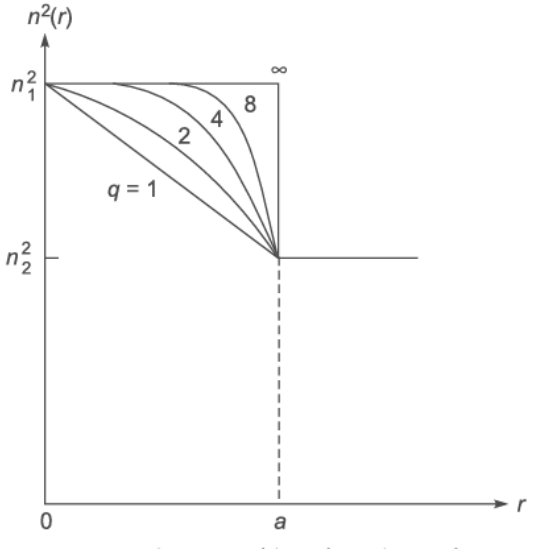

Fig 3.6 Power law profiles for the refractive index distribution

with Δ as defined in Eq. (3.2). The ray paths in a parabolic waveguide are sinusoidal [see Fig 3.7]. For a typical (multimode) parabolic-index silica fiber $\Delta \approx 0.01$, $n_2 \approx 1.45$ and a 25 μm

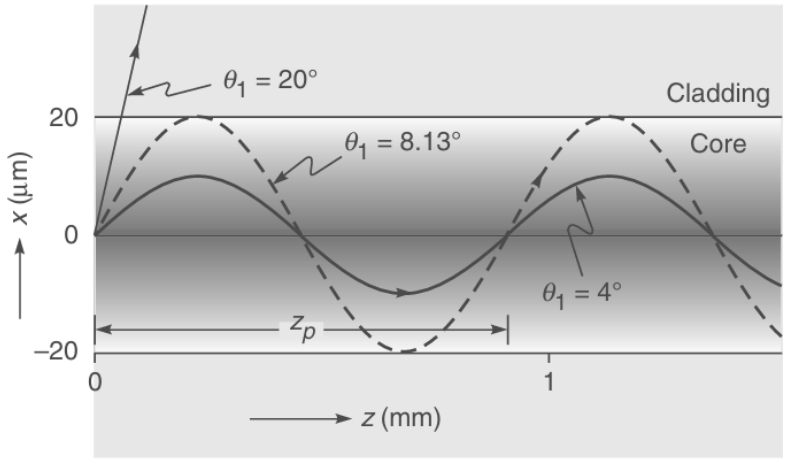

Fig 3.7 Ray paths in a parabolic index fiber.

Now, even though rays making larger angles with the axis traverse a larger path length, they do so now in a region of lower refractive index (and hence greater speed). The longer path length is almost compensated for by a greater average speed such that all rays take approximately the same amount of time in traversing the fiber.

$$\Delta\tau_i = \frac{n_2 L}{2c}\left(\frac{n_1 - n_2}{n_2}\right)^2$$ Pulse dispersion in multimode PIF

When $\Delta << 1$, the above equation can be written as

$$\Delta\tau_i \approx \frac{n_2 L}{2c}\Delta^2 \approx \frac{L}{8cn_1^3}(\mathrm{NA})^4$$

Note that as compared to a step index fiber, the pulse dispersion is proportional to the square of Δ . For a typical (multimode parabolic index) fiber with $n_2 \approx 1.45$ and $\Delta \approx 0.01$, we would get

$$\Delta\tau_i \approx 0.25 \text{ ns/km}$$

$$\Delta\tau_i = \frac{1.5 \times 1000}{3 \times 10^8} \times 0.01 = 50 \text{ ns/km} \quad \ldots\ldots\ldots 3.5$$

Comparing with Eq. (3.5) we find that for a parabolic index fiber the pulse dispersion is reduced by a factor of about 200 in comparison to the step index fiber. It is because of this reason that first and second-generation optical communication systems used near parabolic index fibers. In order to further decrease the pulse dispersion, it is necessary to use single mode fibers because there will be no intermodal dispersion. We must mention that although in almost all long-distance fiber optic communication systems one uses single mode fibers; nevertheless, in many local area communication systems (like intra office networks), one still uses parabolic index multimode fibers. One of the main advantages of using multimode fibers (in

communication networks) is the fact that they have very large core diameters allowing easy splicing at joints. Now, in addition to the intermodal dispersion dis cussed above, in all fiber optic systems we will have material dispersion which is a characteristic of the material itself and not of the waveguide.

Fiber-optic sensors:

Sensors that exploit the optical properties and light guiding capabilities of fibers are called fiber-optic sensors (FOS). In the recent past, there has been tremendous interest in the development of fiber-optic sensors; this is due to high immunity of the optical fiber to electromagnetic interference, applicability to remote sensing, etc. another important attribute is the possibility of having distributed sensing geometries. Fiber optic sensors can be broadly classified into two categories: extrinsic and intrinsic. In the case of extrinsic sensors, the optical fiber simply acts as a device to transmit and collect light from a sensing element, which is external to the fiber. The sensing element responds to the external perturbation and the change in the characteristics of the sensing element is transmitted by the return fiber for analysis. The optical fiber here plays no role other than that of transmitting the light beam. On the other hand, in the case of intrinsic sensors, the physical parameter to be sensed directly alters the properties of the optical fiber, which in turn leads to changes in a characteristic such as intensity, polarization, phase etc. of the light beam propagating in the fiber. We give below descriptions of a few fiber-optic sensors.

Precision displacement sensor

An extrinsic type intensity-based displacement sensor arrangement is shown in Fig. 3.8 As shown in the diagram a GRIN lens is butted with two multimode optical fibres in a Y-splitting configuration. Two 50/125 m fibres enter the probe-head, with one attached to a 680 nm laser-diode source and the other attached to a photodiode detector. In a typical setup, the probe-head is pencil-shaped, 5 mm in diameter and 35 mm in length. A movable reflective surface is used as the transducing device, while a GRIN lens efficiently guides the light between the multimode fibers. The setting-up procedure includes butting the GRIN lens against the fiber ends and aligning the reflective surface with the y-axis of the probe. The lens is manipulated within the x-y plane for maximum detected light, and bonded to the fiber ends using epoxy. Translation and displacement of the reflective surface were allowed along the z-axis. A photograph of a typical fiber-optic displacement sensor (cabled) probe is shown in Fig 3.9. In Fig 3.10. we have shown a typical variation of the detector output with displacement using both plane mirror and polished steel reflectors. The reflector has been moved forward and backward along z-axis using translation stage. The detected optical intensity increases to a maximum value at about 1 mm displacement (the beam waist position) and decreases thereafter giving a usable monotonic displacement-measurement range of at most from about 1 mm to 5.5 mm, indicating a practical working range of some 4.5 mm

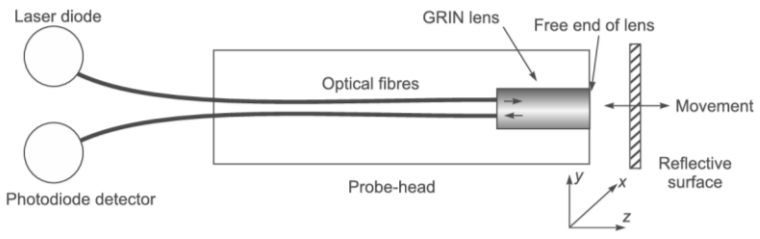

Fig 3.8 Intensity based displacement sensor using two multimode fibers

Fig 3.9 Typical cabled probe used for displacement measurement

Precision vibration sensor

A non-contact vibration-monitoring technique based on transient measurements from a FPI (Fabry Perot Interferometric) displacement sensor is shown in Fig. 3.11. In this scheme one single mode fiber (SMF) is used for both purposes, to inject light input to the sensor and return reflected signal to the detector. A pig-tailed laser diode was spliced to a 50:50 coupler. Back-reflection from the unused coupler port was avoided by immersion in index matching gel. A single SMF was used both to illuminate the sensing element and to collect the reflected signal. In order to guide the input and output light, a gradient index rod (GRIN) lens was butted to the end of the SMF. To provide the interference reference signal, a coating of 25% reflectivity was applied to the output face of the GRIN lens, while a movable reflector (which is to be attached to the vibrating surface being monitored) acts as the second FPI mirror. The FPI has a low finesse of at most 1.34. Light reflected from the GRIN lens mixes coherently with phase modulated light from the movable reflector to produce interference fringes. Now, a monochromatic wave of free-space wavelength λ_0 reflected within an FPI defined by two parallel mirror surfaces, as shown in Fig. 3.11, experiences a round-trip phase-lag given by

$$\phi = \frac{4\pi n d}{\lambda_0}$$

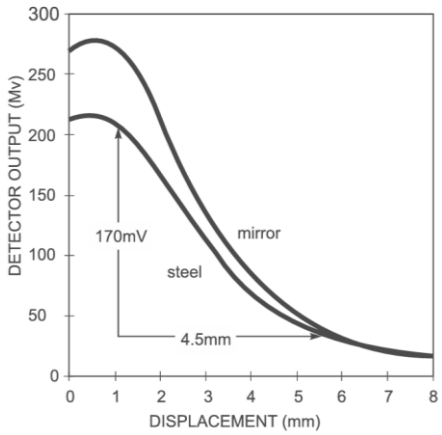

Fig 3.10 Displacement measurement using the plane mirror and polished steel reflectors

where n is the refractive index of the medium between the mirrors, and d is the mirror separation. For vibration measurements, the phase-modulated signal may be derived via reflection from the vibrating surface being monitored, with the reference signal reflected from a static mirror. As one fringe is equivalent to one λ change in optical path difference, for a FPI with a reflective configuration in air (n = 1), it is also equivalent to $\frac{\lambda}{2}$ displacement. If D represents the maximum displacement amplitude from zero position, then the number of fringes counted in half a cycle will be given by

$$N = \frac{D}{\lambda_0/2} \quad \Rightarrow \quad D = \frac{N\lambda_0}{2} \qquad \ldots\ldots\ldots 3.6$$

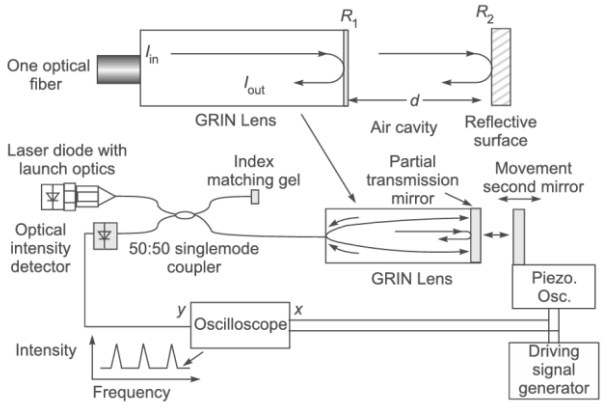

Fig 3.11 Schematic diagram of the FPI sensor system with single-mode fiber

A typical detector output for interferometric precision vibration measurement is shown in Fig 3.12. The figure shows the fringe patterns obtained at low and high amplitude excitation at 1 kHz. The wavelength of the laser diode is 780 nm. At the low excitation there are twenty-two fringes and from Eq. (3.6), we obtain At the high excitation there are 34 fringes, which is equivalent to D = 13.26 m.

$$D = \frac{22 \times 0.78\ \mu\text{m}}{2} = 8.58\ \mu\text{m}$$

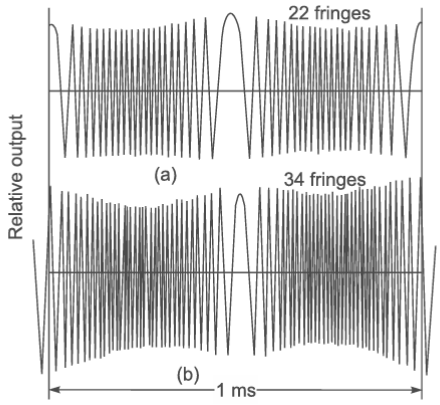

Fig 3.12. 1 kHz response of the EFPI sensor system with one single-mode fiber (a) at 8.58 μm vibration amplitude (≡22 fringes) (b) at 13.26 μm vibration amplitude (≡ 34 fringes)

UNIT – IV
NON-LINEAR OPTICS

Basic principles

Harmonic generation

Non-linear properties in optical region have been strikingly demonstrated by the harmonic generation of light observed for the first time by Franken and coworkers in 1961. They observed ultraviolet light at twice the frequency of a ruby laser light (k = 6493Å), when the light was made to traverse a quartz crystal. This experiment attracted widespread attention and marked the beginning of the experimental and theoretical investigation of nonlinear optical properties. A simplest scheme for this experiment is shown in Fig 4.1.

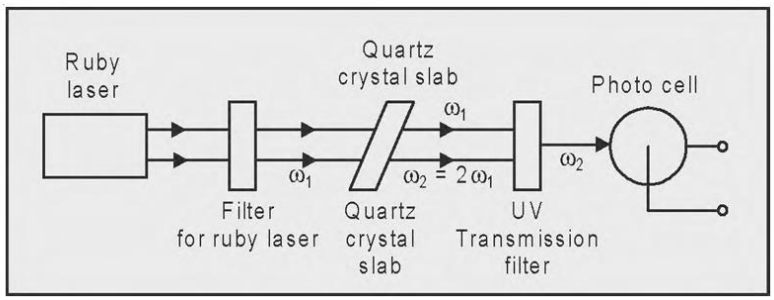

Fig 4.1 Second harmonic generations

A ruby laser beam (k = 6493 Å) with average power of the order of 10 kW is focused on a quartz slab. The transmitted light then was passed through a filter which cuts off the red light and allows uv light to pass through. The emerging light was incident on a photocell. Radiation with wavelength k = 3471 Å and the power of the order of 1 mW was observed in the transmitted light. How can one account for this change in frequency? A dielectric medium when placed in an electric field is polarized, if the medium does not have a transition at the frequency of the field. Each constituent molecule acts as a dipole, with a dipole moment P_i. The dipole moment vector per unit volume P is given by

$$\mathbf{P} = \sum_i \mathrm{P}_i$$

where the summation is over the dipoles in the unit volume. The orienting effect of the external field on the molecular dipoles depends both on the properties of the medium and on the field strength. Thus, we can write

$$\mathbf{P} = \varepsilon_0 \chi \mathbf{E} \quad \ldots\ldots\ldots 4.1$$

where χ is called the polarizability or dielectric susceptibility of the medium. This relation is valid for the field strengths of conventional sources. The quantity χ is a constant only in the sense of being independent of E; its magnitude is a function of the frequency. With sufficiently intense laser radiation the relation (4.1) does not hold good and has to be generalized to

$$P = \varepsilon_0(\chi^{(1)}E + \chi^{(2)}E^2 + \chi^{(3)}E^3 + \ldots) \quad \ldots\ldots\ldots 4.2$$

where $\chi^{(1)}$ is the same as χ in (4.1); the coefficients $\chi^{(2)}$, $\chi^{(3)}$,... define the degree of non-linearity and are known as nonlinear susceptibilities. If the field is low, as it is in the case of ordinary light sources, only the first term of (4.2) can be retained. It is for this reason that the prelaser optics is known as linear optics. Higher the value of the electric field, more significant become the higher order terms. It may be noted that optical characteristics of a medium, such as dielectric permittivity, refractive index, etc., which depend upon susceptibility, also become functions of the field strength E, if it is sufficiently high. The medium of which the polarization is described by a nonlinear relation of the type (4.2) is called a "non-linear medium." Suppose now that the field incident on a medium has the form

$$E = E_0 \cos \omega t.$$

Substituting this in (4.2), we have

$$P = \varepsilon_0\chi^{(1)}E_0 \cos\omega t + \varepsilon_0\chi^{(2)}E_0^2 \cos^2 \omega t + \varepsilon_0\chi^{(3)}E_0^3 \cos^3 \omega t + \ldots \quad \ldots.4.3$$

Using the trigonometric relations

$$\cos^2\theta = \frac{1+\cos 2\theta}{2}; \qquad \cos^3\theta = \frac{\cos 3\theta + 3\cos\theta}{4}$$

we can transform (4.3) to the form

$$P = \frac{1}{2}\varepsilon_0\chi^{(2)}E_0^2 + \varepsilon_0\left(\chi^{(1)} + \frac{3}{4}\chi^{(3)}E_0^2\right)E_0 \cos\omega t$$

$$+ \frac{1}{2}\varepsilon_0\chi^{(2)}E_0^2 \cos 2\omega t + \frac{1}{4}\varepsilon_0\chi^{(3)}E_0^3 \cos 3\omega t + \ldots$$

The first term is a constant term. It gives rise to a dc field across the medium, the effect of which is of comparatively little practical importance. The second follows the external polarization and is called the first or fundamental harmonic of polarization; the third oscillates at frequency 2ω and is called the second harmonic of polarization, the fourth is called the third harmonic of polarization, and so on.

Second harmonic generation

A polarization oscillating at frequency 2ω radiates an electromagnetic wave of the same frequency, which propagates with the same velocity as that of the incident wave. The wave, thus, produced, has the same characteristics of directionality and monochromacity as the incident wave and is emitted in the same direction. This phenomenon is known as the Second Harmonic Generation (SHG). In most crystalline materials, the nonlinear polarizability $\chi^{(2)}$ depends on the direction of propagation, polarization of the electric field and the orientation of the optic axis of the crystal. Since in such crystalline materials the

vectors **P** and **E** are not necessarily parallel the coefficients χ must be treated as tensors. The second order polarization, therefore, may be represented by the relation of the type

$$P_i^{(2)} = \varepsilon_0 \sum_{j,k} \chi_{ijk}^{(2)} E_j E_k \quad \ldots.4.4$$

where i , j, k represent the coordinates x, y, z,. Most of the coefficients χ_{ijk}, however, are usually zero and we have to deal only with one or two components. It must be mentioned here that the second harmonic generation represented by (4.4) occurs only in certain type of crystals. Consider, for example, a crystal that is isotropic. In this case χ_{ijk} is independent of direction and, hence, is a constant. If we now reverse, the direction of the axis (x → - x, y → - y, z →-z) leaving electric field and dipole moment unchanged in direction, the sign of these two must change.

$$-P_i^{(2)} = \varepsilon_0 \sum_{j,k} \chi_{ijk}^{(2)} (-E_j)(-E_k) = +P_i^{(2)}$$

$$P_i^{(2)} = 0 \text{ and, hence, } \chi_{ijk}^{(2)} = 0.$$

Second harmonic generation, therefore, cannot occur in an isotropic medium such as liquids or gases nor in centro-symmetric crystals (i.e., crystals symmetrical about a point). Only crystals that lack inversion symmetry exhibit SHG. In the case of non-centro-symmetric materials (e.g., anisotropic crystals, such as uniaxial crystals) both the quadratic and cubic terms are present. However, generally, the cubic term is sustantially smaller than the second order term and may be ignored. For such materials, we can write

$$P = \varepsilon_0 \chi^{(1)} E + \varepsilon_0 \chi^{(2)} E^2$$

and the medium is said to have second order linearity.

Phase matching

The intense development of research on the mechanism of generation of optical harmonics in crystals and media in which such generation is effectively realizable, has indicated the importance of phase relation between the fundamental and generated harmonics, as they propagate in crystals having optical dispersion. It was observed that the efficiency of the generation of harmonics depends not only on the intensity of the exciting radiation, but also on its direction of propagation in crystals.

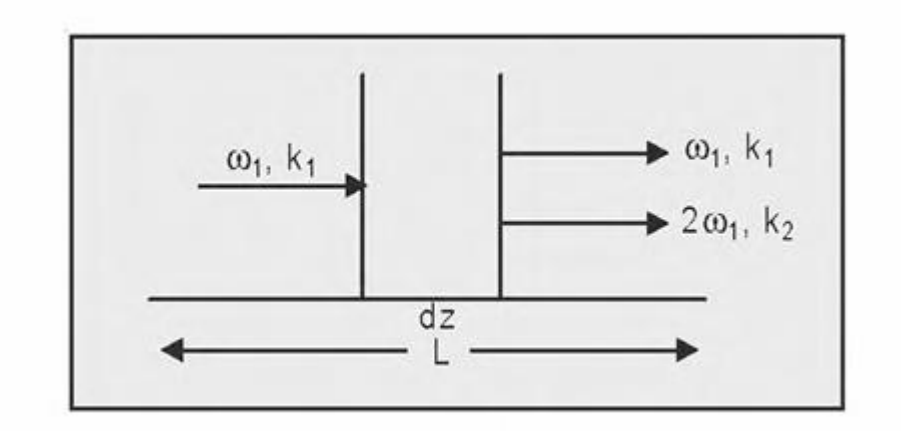

Fig 4.2 Second harmonic wave propagating through a material of length L

Suppose a plane wave at frequency ω and the second harmonic wave at frequency 2ω driven by it are propagating in the z-direction through a material of length L (Fig 4.2). Let us find an expression for the intensity of SHG at the exit surface of the material. The amount of second harmonic radiation produced within a slab of width dz located at z will be proportional to the width and to the second harmonic dipole moment per unit volume induced at frequency 2ω, i.e., $P^2_{(z)}$ which, in turn, is proportional to the square of the electric field E, that is

$$dE^{(2)}_{(z)} \propto P^{(2)}_{(z)} dz \propto \exp(2i(k_1 z - \omega t))dz \ (\because E \propto \exp(i(k_1 z - \omega t))$$

where dE^2_2 is the amount of second harmonic radiation within the slab. We see that the spatial variation of the second harmonic polarization is characterized by a wave member $2k_1$. The second harmonic radiation produced by this slab at the exit surface of the crystal, i.e., at z = L obviously will be

$$dE^{(2)}_{(L)} \propto dE^{(2)}_{(z)} \exp(ik_2(L - z))dz$$

where L - z is the distance from the slab to the end of the crystal and k_2 is the propagation wave number of the second harmonic radiation. In general, $k_2 \neq k_1$ because of dispersion. (Note $k = \frac{2\pi\eta}{\lambda}$)

$$\begin{aligned} dE^{(2)}_{(L)} &\propto \exp(2i(k_1 z - \omega t)) \exp(ik_2 (L - z))dz \\ &= \exp(i(2k_1 - k_2))z \exp(i(k_2 L - 2\omega t))dz \end{aligned} \quad \ldots.4.5$$

We have assumed here that the incident power is nearly unchanged as the beam propagates through the crystal.

Integrating (4.5)

$$E_{(L)}^{(2)} \propto \int_0^L \exp\,(i(2k_1 - k_2)z)\,\exp\,(i(k_2 L - 2\omega t))dz$$

$$= \frac{\exp(i(k_2 L - 2\omega t)\,[\exp(i(2k_1 - k_2)L) - 1]}{i(2k_1 - k_2)}$$

On simplification and some manipulation, we get

$$E_{(L)}^{(2)} \propto \frac{\sin\left(\frac{2k_1 - k_2}{2}\right)L}{\left(\frac{2k_1 - k_2}{2}\right)}$$

where we have taken only the real part of the proportionality factor.

This will be maximum when $\frac{(2k_1 - k_2)}{2} = \frac{\pi}{2}$, that is, the field of the 22 second harmonic generation will be maximum when

$$L = \frac{\pi}{2k_1 - k_2} = \frac{\lambda}{4(\eta_\omega - \eta_{2\omega})} \quad \ldots.4.6$$

where η_ω, $\eta_{2\omega}$ are the refractive indices at ω and 2ω respectively.

Increasing L beyond this value will not result into any increase in $E^{(2)}$. The magnitude of L given by (4.6) is called the coherence length for the second harmonic radiation.

The expression for intensity, viz.

$$I \propto \frac{\sin^2\left(\frac{2k_1 - k_2}{2}\right)L}{\left(\frac{2k_1 - k_2}{2}\right)^2}$$

is sharply peaked about

$$\left(\frac{2k_1 - k_2}{2}\right)L = 0$$

$$k_2 = 2k_1$$

For efficient frequency doubling, this relation must be satisfied. This requirement is known as phase-matching criterion.

$$k_2 = \frac{2\omega\eta_{2\omega}}{c} \quad \text{and} \quad k_1 = \frac{\omega\eta_\omega}{c}$$

relation (13.18) reduces to

$$\eta_{2\omega} = \eta_{\omega}.$$

Thus, the phase matching criterion becomes a refractive-index criterion. It is rather difficult to fulfill this requirement because most materials show some sort of dispersion in the refractive index. A satisfactory solution to this problem would be to use the dependence of the refractive index on the direction in anisotropic crystals. A birefringent material has different refractive indices for different polarization of light. This occurs generally in crystals of low symmetry. A light wave entering an anisotropic crystal split into two waves travelling at different velocities. In uniaxial crystals the ray corresponding to the wave whose refractive index is independent of the direction of propagation is called the ordinary ray

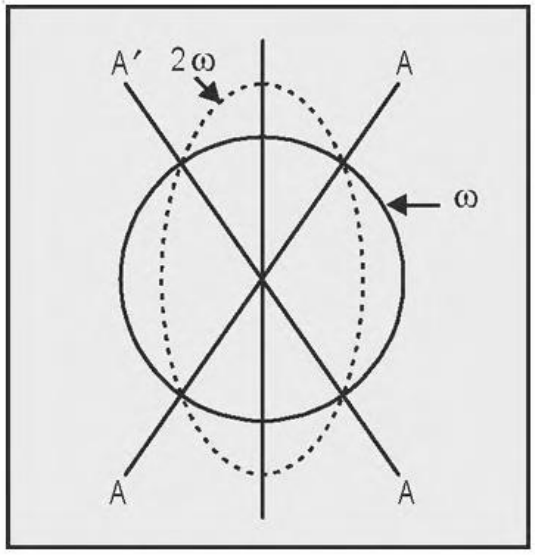

Fig 4.3 Indicatrix for a negative uniaxial crystal

Third harmonic generation

As stated in Second harmonic generation, in the case of centrosymmetric materials, the expression (4.2) will lack terms in even powers of E and it will reduce to

$$P = \varepsilon_0\chi^{(1)}E + \varepsilon_0\chi^{(3)}E^3 + \ldots$$

Or in vector notation

$$P = \varepsilon_0\chi^{(1)}E + \varepsilon_0\chi^{(3)}E^2E + \ldots$$

Third harmonic generation (THG) is, therefore, possible in crystals that exhibit inversion symmetry. The development of Q-switched lasers had made it possible to generate third harmonic in crystals. However, the energy conversion efficiency in such cases is very low. For example, in calcite the maximum energy conversion efficiency in the third harmonic was 0.01%. Experiments for observation of the third harmonic were also performed by Maker and Terhune using giant pulse lasers. Zwernemann and Beeker have observed experimentally the enhancement of third harmonic generation (THG) at 9.33 μm in CO by having the

interaction take place in a waveguide. They have presented a theoretical determination of the most suitable waveguide in which the interaction can take place. The process of generation of higher order harmonics can be explained on the same lines

Optical mixing

In the equation for nonlinear polarization (4.2), we have assumed that the factor E^2 in the second term, is the product of the electric field strength with itself, E.E. However, such a nonpolarization term may also result from the interaction of two fields with different frequencies. Suppose two coherent light wave trains of unequal frequencies ω_1 and ω_2 are traversing the material. The effective field in the material is

$$E = E_1 \cos \omega_1 t + E_2 \cos \omega_2 t$$

Substituting this in (4.2), the second term becomes

$$\begin{aligned} P^{(2)} &= \varepsilon_0 \chi^{(2)} (E_1 \cos \omega_1 t + E_2 \cos \omega_2 t)^2 \\ &= \varepsilon_0 \chi^{(2)} (E_1^2 \cos^2 \omega_1 t + E_2^2 \cos^2 \omega_2 t) \\ &\quad + 2\varepsilon_0 \chi^{(2)} E_1 E_2 \cos \omega_1 t \cos \omega_2 t \end{aligned} \quad \ldots.4.7$$

Using the trigonometric relation

$$2\cos \alpha \cos \beta = \cos (\alpha + \beta) + \cos (\alpha - \beta)$$

We can express the last term as

$$\begin{aligned} &2\varepsilon_0 \chi^{(2)} E_1 E_2 \cos \omega_1 t \cos \omega_2 t \\ &\quad = \varepsilon_0 \chi^{(2)} E_1 E_2 [\cos (\omega_1 + \omega_2) t + \cos (\omega_1 - \omega_2) t] \end{aligned} \quad \ldots4.8$$

This shows that the non-linear polarization and, therefore, emitted radiation contains frequencies $\omega_1 + \omega_2$ and $\omega_1 - \omega_2$. The energy conversion between the beams can take place over significant distances only if the beams travel in the same direction and at the same velocity. The sum and difference frequencies can be observed experimentally. Generation of difference optical frequencies was first observed by mixing a beam from a ruby laser with an incoherent beam of a mercury lamp (k = 3115 Å). The efficiency with which the difference frequency was generated was negligible; with the power in the mercury beam amounting to about 2×10^{-4} W, the power radiated at the difference frequency was 10^{-10} W. Optical mixing of the emission, of two ruby lasers with different frequencies. The first term of (4.7), besides frequency doubling, also leads to a dc term. In the case of second harmonic generation, it is necessary to find a direction in crystals such that $k_1 = k_2$. In the case of sum or difference frequencies, three waves must be matched. If

$$\omega_3 = \omega_1 \pm \omega_2,$$

the condition to be satisfied is

$$k_3 = k_1 \pm k_2$$

Parametric generation of light

Parametric phenomena in electronics are widely known. They occur in circuits involving nonlinear capacitors. Similar processes occur in optics when nonlinear crystals are used as parametric media. The process is known as parametric generation of light, and is based on "optical mixing" discussed in the preceding section. Suppose a powerful signal at frequency ω_p(pump frequency) is applied to a parametric medium and a small signal at frequency ω_s (signal frequency) is introduced at one end. The fields at the original frequencies are regarded as fixed parameters. "Mixing" of the signal and the pump frequency may result into a secondary wave at frequency ω_i given by

$$\omega_i = \omega_p - \omega_s$$

which is known as 'idler' frequency. The corresponding field strength being proportional to

$$E_p E_s = E_i \quad \ldots.4.9$$

as shown by equation (4.8).

In view of the non-linear properties of the medium, further mixing may occur. In particular, the field generated by the polarization component oscillating at the idler frequency and the original pump field, when mixed, would make a contribution to the signal field. Thus

$$\omega_p - \omega_i = \omega_p - (\omega_p - \omega_s) = \omega_s.$$

The strength of the contribution is proportional to

$$E_p E_i = E_p^2 E_s$$

where we have used (4.9). This shows that the strength is proportional to E_s, in accordance with the usual requirement for parametric amplification. Thus, the secondary light waves at frequencies ω_s and ω_i can be excited parametrically at the expense of the part of energy of the pumping wave. Initial signals required for triggering the process of parametric generation are always available in any crystal in the form of spontaneous photons.

Self-focusing of light.

The refractive index of a material is related to the susceptibility by the relation.

$$\eta = \sqrt{1 + \chi}$$

Since the susceptibility % is a function of the field E, n depends on E. This dependence of the refractive index on the field strength gives rise to a nonlinear effect: self-focusing of intense light beams. Self-focusing does not alter the frequency of the light waves. We need, therefore, consider only the second term in the relation (13.7) which describes the

fundamental harmonic, viz.

$$P^{(1)} = \varepsilon_0(\chi^{(1)} + \frac{3}{4}\chi^{(2)} E_0^2)E.$$

The expression for the refractive index consequently is

$$\eta = \sqrt{1 + (\chi^{(1)} + \frac{3}{4}\chi^{(2)}E_0^2)}$$

We write this as

$$\eta = \sqrt{\varepsilon_l + \varepsilon_{nl}}$$

where we have put

$$\varepsilon_l = 1 + \chi^{(1)}$$

which gives the dielectric permittivity of the linear medium, and

$$\varepsilon_{nl} = \frac{3}{4}\chi^{(2)}E_0^2$$

is a non-linear increment in the expression for dielectric permittivity.

$$\eta = \sqrt{\varepsilon_l}\sqrt{1 + \frac{\varepsilon_{nl}}{\varepsilon_l}} \approx \sqrt{\varepsilon_l}\left(1 + \frac{\varepsilon_{nl}}{2\varepsilon_l}\right)$$

$$(\because \varepsilon_{nl} << \varepsilon_l)$$

$$= \eta_l\left(1 + \frac{\varepsilon_{nl}}{2\eta_l^2}\right) = \eta_l\left(1 + \frac{3\chi^{(2)}E_0^2}{8\eta_l^2}\right)$$

Or

$$\eta = \eta_l\,(1 + \eta_{nl}E_0^2)$$

where $\eta_l = \sqrt{\varepsilon_l}$ is the refractive index of the linear medium, and

$$\eta_l\eta_{nl}E_0^2 = \frac{\varepsilon_{nl}}{2\sqrt{\varepsilon_l}} = \frac{3\chi^{(2)}E_0^2}{8\sqrt{1 + \chi^{(1)}}}$$

is the non-linear increment in the expression for the refractive index. We, thus, see that the refractive index of a non-linear medium is proportional to the square of the amplitude of the field, that is, to the intensity. Now the intensity of a laser beam is not constant over its cross-section. It peaks at the axis of the beam and falls off gradually away from the axis. The velocity of the light wave is given by v = c / η. Since η decreases owing to the falling of the intensity of the light beam, the velocity increases with the distance away from the axis. Consequently, a plane wave-front incident on material becomes concave as it propagates through the medium and contracts towards the axis (Fig. 4.4). In other words, it self-focusses, after which it propagates as a narrow light fiber.

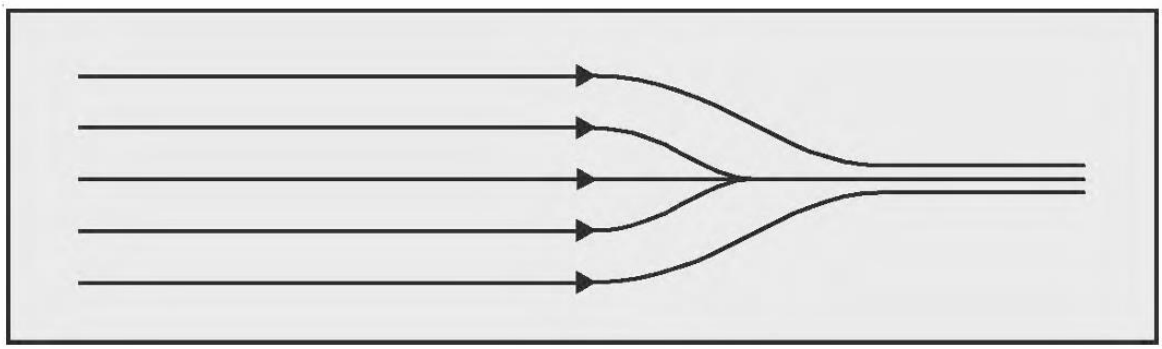

Fig 4.4 Self-focusing

The distance L_0 over which the beam self-focusses can be approximately estimated using the formula,

$$L_0 = \frac{D}{\sqrt{\eta_{nl} E_0^2}}$$

where D is the diameter of the beam. Self-focusing occurs when intensity reaches a certain limiting value. This threshold value is estimated from the formula

$$I_{\text{thresh}} = \frac{\lambda^2}{\eta_l^2 \eta_{nl} D^2}$$

The formula shows that for higher frequencies and for materials with greater non-linear susceptibilities, the threshold intensity is lower. Experimental investigations in self-focusing have been carried out in liquids: Carbon sulphide, benzene, acetone, etc., For a beam diameter of 0.5 μm, the self-focusing distance, is about 10 cm and the observed light fibres were 30 to 50 μm, in diameter. It has been further established that the observed light fiber has still a finer structure; it consists of a number of still thinner filaments with diameters of about 5 μm. Self-focusing, on the whole, is a complicated phenomenon.

UNIT – V
MAGNETO- OPTICS AND ELECTRO-OPTICS

Magneto - optical effects

Magneto-optical effects refer to phenomena in which the interaction between light (optical radiation) and a magnetic field result in changes to the properties of the light itself or to the material through which it passes. These effects arise due to the influence of the magnetic field on the behavior of charged particles (such as electrons) and their associated magnetic moments within the material.

Zeeman effect

Zeeman effect is a magneto-optical phenomenon discovered by Zeeman in 1896. If a source of light producing line spectrum is placed in a magnetic field, the spectral lines are split into components. This phenomenon is called Zeeman effect. They are of two kinds,

- Normal Zeeman effect and
- Anomalous Zeeman effect.

Experimental study of Zeeman effect.

The arrangement is as shown in the diagram. MM is a strong electromagnet which produces strong magnetic field. Its conical pole pieces PP have longitudinal holes drilled through them. A source of light L (say sodium vapour lamp) producing line spectrum is placed between the pole pieces. The spectral lines are observed with the help of a spectrograph S of high resolving power. The Zeeman effect is observed in two ways.

1. The spectral line is viewed without the application of magnetic field. Now the magnetic field is applied and the spectral line is viewed longitudinally through the hole drilled in the pole pieces and hence parallel to the direction of the magnetic field. The spectral line is found to split into two components one with the longer wavelength and the other with the shorter wavelength than the original line. The original line is absent. These two lines are symmetrically situated on either side of the original line. Analyzing the two lines with the Nicol prism, both are found to be circularly polarized in opposite directions. This is called **Normal longitudinal Zeeman effect**.
2. When the spectral line is viewed along the transverse direction, i.e. perpendicular to the magnetic field, it is found to split in to three components. The central line has the same wavelength as that of the original line and is plane polarized with the vibrations parallel to the direction of the field. The outer lines are symmetrically positioned about the central line and both these lines are plane polarized with the vibrations perpendicular to the magnetic field. The displacement of the either of the two outer lines from the central line is called Zeeman shift. This is called **Normal transverse Zeeman effect.**

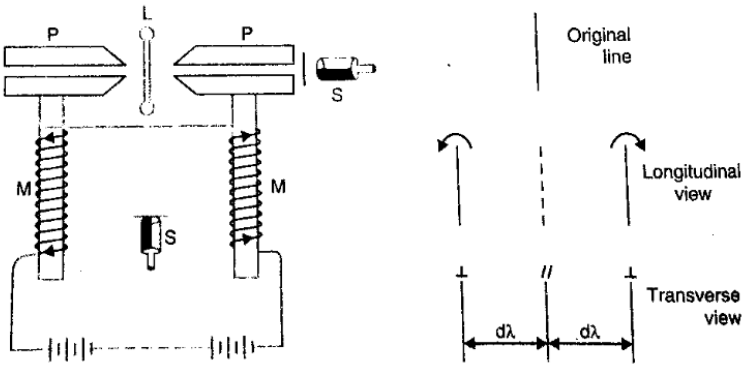

Fig 5.1 Zeeman effect experimental setup.

Normal Zeeman Effect

The splitting of a spectral line into two or three components in a magnetic field is called the Normal Zeeman effect. The experimental arrangement is explained above. Debye explained the Normal Zeeman effect without taking into account the concept of electron spin. By neglecting the spin motion, the orbital angular momentum of the electron is

$$p_l = \frac{lh}{2\pi} \quad .....(1)$$

The magnetic moment is given by

$$\mu_l = \frac{e}{2m} p_l \quad .....(2)$$

In the presence of an external magnetic field of flux density B, the vector l precesses around the direction of magnetic field as the axis. This precession is the Larmor precession. The potential energy of the electron due to interaction between orbital magnetic moment and the magnetic field B is given by

$$U_m = -\mu_l . B$$

If θ is the angle between B and p_l, then μ_l has a direction opposite to p_l, thus

$$U_m = \mu_l B \cos\theta \quad ...(3)$$

The frequency of the Larmor precession is

$$\omega = \frac{Be}{2m} \quad .....(4)$$

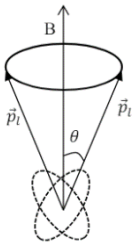

Fig 5.2 Electronic orbit

The diagram Fig 5.2 shows two positions of the vector pl as it precesses about the electronic

orbit. The effect of this precession is to change the energy of the system by an amount ΔE which is the potential energy gained by the electron, given by

$$\Delta E = \mu_l B \cos\theta \quad ....(5)$$

Substituting (2) and (1) in (5)

$$\Delta E = \frac{e}{2m} p_l B \cos\theta = \frac{e}{2m} \frac{lh}{2\pi} B \cos\theta$$

$$\Delta E = \frac{Be}{2m} \frac{h}{2\pi} l \cos\theta$$

But $\frac{Be}{2m} = \omega$

and $l \cos\theta$ is the projection of l on B = m_l.

$$\Delta E = m_l \frac{eh}{4\pi m} B = m_l \omega \frac{h}{2\pi} \quad .....(6)$$

Now ml can have $(2l + 1)$ values from $+l$ to $-l$. Therefore, an external magnetic field will split a single energy level into $(2l + 1)$ levels. The d - state (l = 2) is split into 5 sublevels and the p – state (l = 1) is split in to 3 sublevels as shown. Let $E_0{}'$ be the energy of the level l = 1 in the absence of magnetic field and EB' be the energy of this level in the presence of the field.

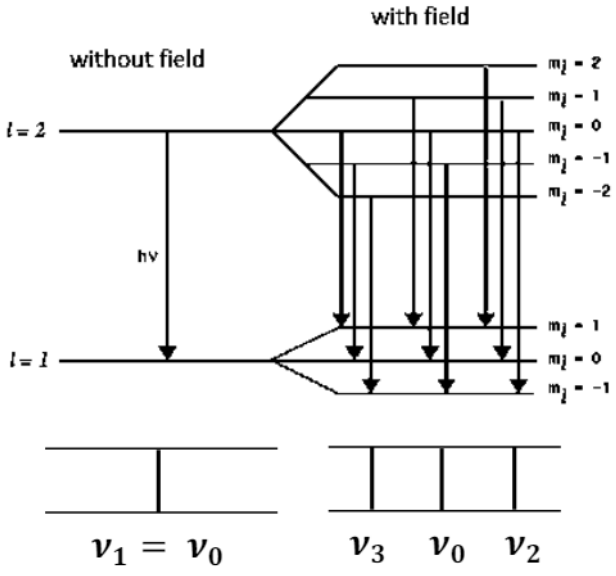

Fig 5.3 Zeeman effect spectral line splitting

$$E_B' = E_0' + \Delta E' = E_0' + m_l' \frac{eh}{4\pi m} B \ldots(7)$$

Let $E0''$ be the energy of the level l = 2 in the absence of magnetic field and EB'' be the energy of this level in the presence of the field. Then

$$E_B'' = E_0'' + \Delta E'' = E_0'' + m_l'' \frac{eh}{4\pi m} B \quad \ldots(8)$$

The quantity of radiation emitted in the presence of magnetic field is

$$E_B'' - E_B' = (E_0'' - E_0') + (m_l'' - m_l') \frac{eh}{4\pi m} B$$

$$\text{or} \quad h\nu = h\nu_0 + \Delta m_l \frac{eh}{4\pi m} B$$

$$\text{or} \quad \nu = \nu_0 + \Delta m_l \frac{eB}{4\pi m} \quad \ldots(9)$$

where ν is the frequency of radiation emitted in the presence of magnetic field and ν_0 is the frequency of emitted radiation in the absence of field. The selection rule for ml is $\Delta m_l = 0$ *or* ± 1. Hence, we have three possible lines. They are

$$\boldsymbol{\nu_1 = \nu_0} \quad \textbf{for} \quad \boldsymbol{\Delta m_l = 0} \quad \textbf{....(10)}$$

$$\boldsymbol{\nu_2 = \nu_0 + \frac{eB}{4\pi m}} \quad \textbf{for } \boldsymbol{\Delta m_l = +1} \quad \textbf{....(11)}$$

$$\boldsymbol{\nu_3 = \nu_0 - \frac{eB}{4\pi m}} \quad \textbf{for} \quad \boldsymbol{\Delta m_l = -1} \quad \ldots\ldots(12)$$

The diagram above represents Normal Zeeman effect. Although there are nine possible transitions, they are grouped into only three different frequency components as indicated by equations (10), (11) and (12). The frequency shift is given by

$$d\nu = \pm \frac{eB}{4\pi m}$$

$$\text{As} \quad \nu = \frac{c}{\lambda}, \quad d\nu = -c \frac{d\lambda}{\lambda^2} \quad \text{or} \quad d\lambda = -\frac{\lambda^2}{c} d\nu$$

Thus, the Zeeman shift in terms of wavelength is

$$\boldsymbol{\Delta\lambda = d\lambda = \pm \left(\frac{\lambda^2}{c}\right) \frac{eB}{4\pi m}}.$$

Inverse Zeeman effect

The inverse Zeeman effect is a phenomenon in atomic and molecular physics that occurs when the spectral lines of an atom or molecule split into multiple components in the presence of an external magnetic field. It is called "inverse" because it involves transitions between different electronic energy levels, as opposed to the normal Zeeman effect, which primarily involves transitions between different angular momentum states.

In the inverse Zeeman effect, the splitting of spectral lines is caused by the interaction of the external magnetic field with the electronic structure of the atom or molecule. Specifically, the magnetic field causes mixing between different electronic states, leading to a modification of the energy levels and resulting in the splitting of spectral lines.

Unlike the normal Zeeman effect, where the splitting is primarily due to the interaction of the magnetic field with the orbital angular momentum and spin of electrons, the inverse Zeeman effect involves transitions between excited states and the ground state of the atom or molecule. As a result, the spectral lines split into multiple components, with some transitions showing a decrease in energy (lower frequency) and others showing an increase in energy (higher frequency) compared to the unsplit line.

The inverse Zeeman effect is observed in various experimental setups, including spectroscopic studies of atoms and molecules in the presence of strong magnetic fields. It provides valuable information about the electronic structure and energy levels of the system under investigation, as well as insights into the behavior of matter in magnetic fields.

Faraday effect

The oldest and best-known MO effect is the Faraday effect, also called magnetic circular birefringence (see Fig 5.4). A magnetic field is applied to a sufficiently trans parent sample parallel to the propagation direction of linearly polarized light. After having passed through the sample, the plane of polarization of the light is rotated by an angle θ_F, which we call the Faraday rotation. If the sample exhibits absorption the emergent light will generally be elliptically polarized. Then, θ_F designates the rotation of the semimajor axis relative to the initial polarization direction and the ratio of the two semiaxes of the ellipse is defined as the tangent of the Faraday ellipticity, tan(ηF).

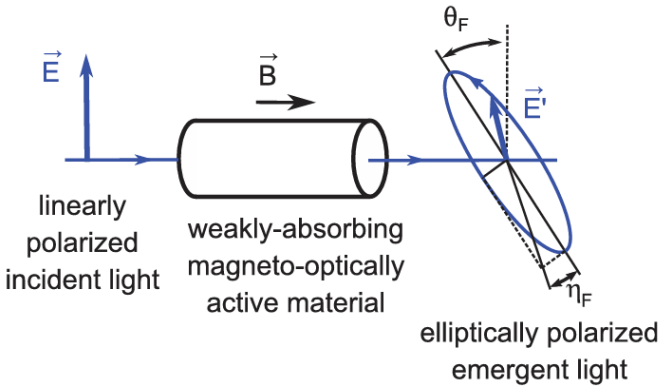

Fig 5.4 Faraday effect

As we will learn later, linearly polarized light can be viewed as a combination of a right and a left circularly polarized wave. Keeping that in mind, a rotation θ_F is equivalent to a phase shift between the two circularly polarized partial waves or to a different propagation velocity of the two partial waves. θ_F is proportional to the difference between the refractive index of right and left circularly polarized light. The difference is, in turn, proportional to the applied magnetic field. In this context, it should be mentioned that there are many molecules that, being in solution, rotate the polarization direction of the light without having a magnetic field applied. This property is called optical activity and has nothing to do with magnetism. It occurs only in chiral materials or molecules, that is, materials or molecules having no mirror symmetry.

Voigt effect

If the magnetic field is applied perpendicular to the propagation direction of the light, the so-called Voigt effect can be observed, also known as transverse or linear magnetic birefringence. It has a sizable magnitude mainly in the immediate vicinity of sharp absorption lines. Through the action of the magnetic field, the refractive index for light polarized parallel to the magnetic field is not altered. For light polarized perpendicular to it, a spectral splitting of the absorption lines is observed. As a result (of a rather lengthy calculation), light which is linearly polarized at an angle of 45° to the magnetic field experiences a phase shift which is proportional to the difference between the refractive index of light polarized parallel and perpendicular to the magnetic field and proportional to the traveled distance. The emerging light is then elliptically polarized with the semimajor axis along the direction of the input polarization. The difference of the refractive index is proportional to the square of the applied magnetic field. In case of absorption, we find a rotation of the polarization plane, too.

Cotton-mouton effect

Using the same geometry as in the Voigt effect, Aimé Cotton and Henri Mouton observed 1907 in certain liquids an effect, which is expressed in the same way with respect to change of polarization and field dependence as the Voigt effect. The origin of this so-called Cotton–Mouton effect is found in the alignment of magnetically anisotropic molecules within a magnetic field. When the molecules are also optically anisotropic, the alignment leads to a birefringence of the liquid in a homogeneous magnetic field. The relationship with the electro-optical Kerr effect is that both have as a condition optically anisotropic molecule. The difference, however, is that in the first case a magnetic anisotropy of the molecules is necessary and in the other case an electrical

Kerr magneto- optic effect

If linearly polarized light is reflected from the specular surface of magnetic materials, the reflected light will in general be elliptically polarized as shown in Fig 5.5. This effect is named Kerr effect after its discoverer. Here, we define the deviation of the semimajor axis of the polarization ellipse from the direction of the incident polarization as the Kerr rotation θ_K and the ratio of the two semiaxes as the tangent of the Kerr ellipticity η_K

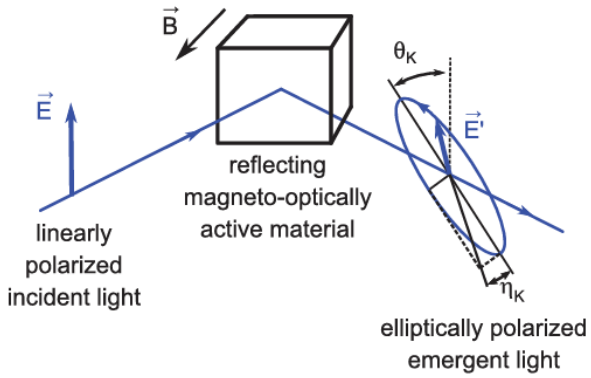

Fig 5.5 polar Kerr effect

Depending on the geometry, three different Kerr effects can be distinguished as plot ted in Fig 5.6. For the polar Kerr effect, the magnetic-field direction or the magnetization is perpendicular to the sample surface and within the plane of incidence of light. For the longitudinal Kerr effect, the magnetic field direction is also within the plane of incidence of light but parallel to the surface of the sample. For the transversal (also called transverse or equatorial) Kerr effect finally, the magnetic field direction is perpendicular to the plane of incidence of light and parallel to the sample surface.

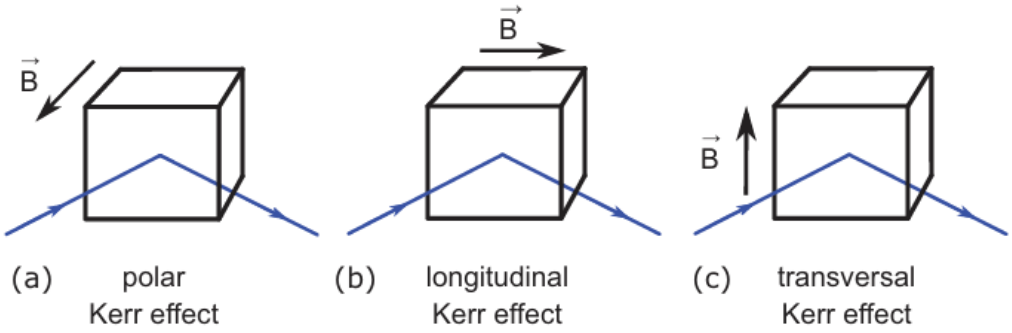

Fig 5.6 (a) polar Kerr effect, (b) longitudinal Kerr effect, and (c)transversal Kerr effect.

The polar geometry is most widely used since it establishes a direct connection with the Faraday effect and because it is the largest effect of the three. If no need for wavelength-dependent measurements exists, for example, taking MO hysteresis curves at a fixed photon energy of the light, then the other geometries are often advantageous since they are much easier accomplished experimentally. The longitudinal Kerr effect is, despite being a small effect, very useful for studying hysteresis curves in thin films because the easy axis of magnetization is usually in plane. A polar Kerr hysteresis curve would then not show a hysteresis because it is only sensitive to the hard axis component of magnetization. For normal incidence of the light, the longitudinal Kerr effect merges toward the transversal. Then it occurs that light polarized parallel to the magnetic field is reflected without change. At grazing incidence, the longitudinal Kerr effect resembles the polar one at perpendicular incidence because the light direction becomes parallel to the magnetic field direction. We will use a simple argument to show these similarities between polar and longitudinal Kerr effect. Of course, the argument is very heuristic because of the different reflectivity at grazing incidence as opposed to normal incidence. Magnetic field introduces a true anisotropy in the material in a plane perpendicular to the magnetic field direction. Therefore, the anisotropy of the surface in the polar Kerr geometry differs from the anisotropy in the longitudinal and transversal Kerr geometry. This re quires a different treatment for each Kerr effect. In this book, we limit ourselves to the discussion of the Faraday effect and the polar Kerr effect at normal incidence

Electro-optical effects

Electro optic effect can be observed when light propagates through a crystal in the presence of an Electric Field. The electric field applied to the crystal can alter or induce birefringence by changing the refractive index of the medium. This effect is known as electro optic effect.

Stark effect

The Stark Effect is shown in Fig 5.7. Splitting and shifting of spectral lines in hydrogen under the influence of an external electric field. The stark effect is the shifting and splitting

(reduction of degeneracy) of spectral lines in atomic or molecular species under the influence of an externally applied electric field. It is sometimes considered the electric analog to the reduction of degeneracy in atomic and molecular species due to an externally applied magnetic field, the Zeeman effect. I'm not fond of that characterization since the two phenomena are quite different, but it is a reasonable viewpoint.

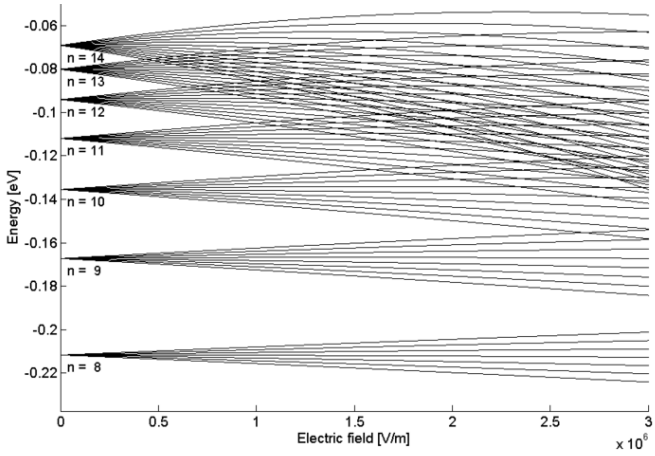

Fig 5.7 Stark effect

There are actually two types of stark effect: the linear stark effect and the quadratic version of the stark effect. As expected, the linear stark effect is linearly dependent on the applied electric field while the quadratic stark effect is smaller in the value of splitting and varies as the square of the applied electric field.

Inverse stark effect

The inverse Stark effect is a phenomenon in atomic and molecular physics that occurs when the energy levels of an atom or molecule are perturbed by an external electric field. It is the opposite of the normal Stark effect.In the normal Stark effect, the energy levels of an atom or molecule split in the presence of an electric field due to the interaction between the electric field and the electric dipole moment of the system. This splitting results in shifts in the energy levels, leading to changes in the spectral lines observed in the system.

Conversely, in the inverse Stark effect, the energy levels of the atom or molecule are perturbed in such a way that they converge rather than diverge as a result of the external electric field. This convergence of energy levels occurs when the external electric field induces mixing between different electronic states, leading to a reduction in the energy differences between these states. The inverse Stark effect is typically observed in systems where the external electric field influences the electronic structure, such as in atoms with high angular momentum or in highly polar molecules. It is important in fields such as spectroscopy and quantum chemistry, where it provides insights into the behavior of atoms and molecules in the presence of electric fields.

Electric double refraction

Birefringence is formally defined as the double refraction of light in a transparent, molecularly ordered material, which is manifested by the existence of orientation-dependent differences in refractive index. Many transparent solids are optically isotropic, meaning that

the index of refraction is equal in all directions throughout the crystalline lattice. Examples of isotropic solids are glass, table salt (sodium chloride, illustrated in Figure 5.8(a), many polymers, and a wide variety of both organic and inorganic compounds.

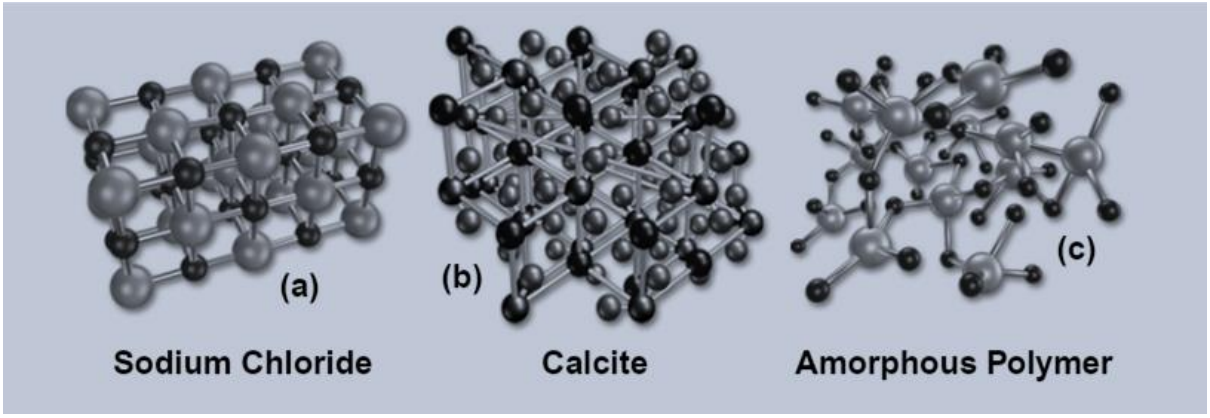

Fig 5.8 Crystalline Structure of Isotropic and Anisotropic Materials

he simplest crystalline lattice structure is cubic, as illustrated by the molecular model of sodium chloride in Figure 5.8 (a), an arrangement where all of the sodium and chloride ions are ordered with uniform spacing along three mutually perpendicular axes. Each chloride ion is surrounded by (and electrostatically bonded to) six individual sodium ions and vice versa for the sodium ions. The lattice structure illustrated in Figure 5.8 (b) represents the mineral calcite (calcium carbonate), which consists of a rather complex, but highly ordered three-dimensional array of calcium and carbonate ions. Calcite has an anisotropic crystalline lattice structure that interacts with light in a totally different manner than isotropic crystals. The polymer illustrated in Figure 5.8 (c) is amorphous and devoid of any recognizable periodic crystalline structure. Polymers often possess some degree of crystalline order and may or may not be optically transparent.

Crystals are classified as being either isotropic or anisotropic depending upon their optical behavior and whether or not their crystallographic axes are equivalent. All isotropic crystals have equivalent axes that interact with light in a similar manner, regardless of the crystal orientation with respect to incident light waves. Light entering an isotropic crystal is refracted at a constant angle and passes through the crystal at a single velocity without being polarized by interaction with the electronic components of the crystalline lattice.

The term anisotropy refers to a non-uniform spatial distribution of properties, which results in different values being obtained when specimens are probed from several directions within the same material. Observed properties are often dependent on the particular probe being employed and often vary depending upon the whether the observed phenomena are based on optical, acoustical, thermal, magnetic, or electrical events. On the other hand, as mentioned above, isotropic properties remain symmetrical, regardless of the direction of measurement, with each type of probe reporting identical results.

Anisotropic crystals, such as quartz, calcite, and tourmaline, have crystallographically distinct axes and interact with light by a mechanism that is dependent upon the orientation of the crystalline lattice with respect to the incident light angle. When light enters the optical axis of anisotropic crystals, it behaves in a manner similar to the interaction with isotropic crystals, and passes through at a single velocity. However, when light enters a non-equivalent axis, it is refracted into two rays, each polarized with the vibration directions oriented at right angles

(mutually perpendicular) to one another and traveling at different velocities. This phenomenon is termed double refraction or birefringence and is exhibited to a greater or lesser degree in all anisotropic crystals.

Kerr electro – optic effect

In Kerr effect, the change in the refractive index is proportional to the square of the applied electric field.

$$\mu = f(E^2)$$

Since the change is very small, by using tailor's series, it can be written as

$$\mu(E) = \mu_0 - \tfrac{1}{2} s \mu^3 E^2$$

The change, $\Delta\mu = \tfrac{1}{2} s \mu^3 E^2$ (s varies from 10^{-18} to 10^{-14} m^2/V^2)

The Kerr effect is very weak compared with pockel. Some highly transparent crystals show Kerr effect but with smaller Kerr constant. Some polar liquids such as Nitro toluene and nitro benzene show appreciable Kerr value. The change in the refractive index induces or alters the birefringence of the crystal and therefore the beam suffers a phase shift. Even though the change in the refractive index is very small, the corresponding phase change in the beam propagating along the direction of applied field could be significant.

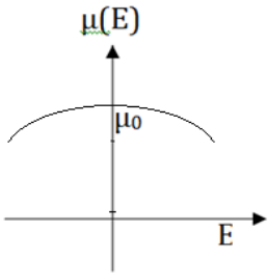

Fig 5.9 Kerr effect

Pockels electro-optic effect.

Pockels effect is observed only in non-centrosymmetric materials. The change in the refractive index ($\Delta\mu$) is proportional to the applied electric field (E)

$$\mu = f(E)$$

Since the change is very small, by using tailor's series, it can be written as

$$\mu(E) = \mu_0 - \tfrac{1}{2} r \mu^3 E$$

The change $\Delta\mu = \tfrac{1}{2} r \mu^3 E$

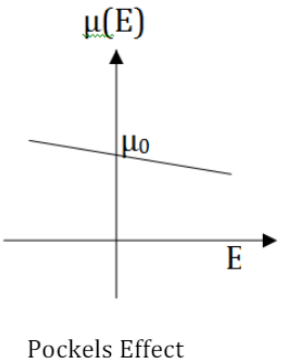

Fig 5.10 Pockels effect

Where r is a constant for a crystal and it varies from 10^{-12} to 10^{-10} m/V.